Fall 2014 NCNR Low-Q Seminar Series

Determination of the Structure of Biological Molecules by SANS and Neutron Reflectometry

(in particular for proteins which cannot be crystallized)

Wednesday, 15 October

Can reference structures be employed in SANS in a way analogous to that used in specular neutron reflectometry?

Chuck Majkrzak

6/26/13 ferritin1.jpg

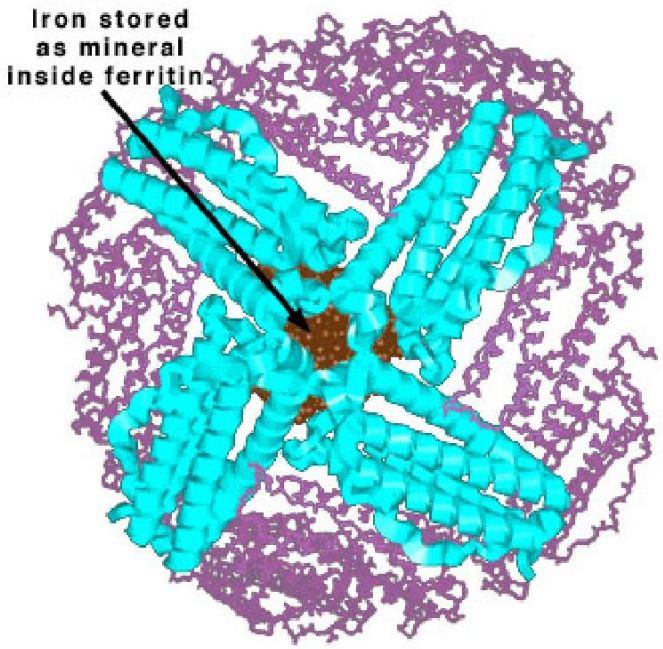

www.chemistry.wustl.edu

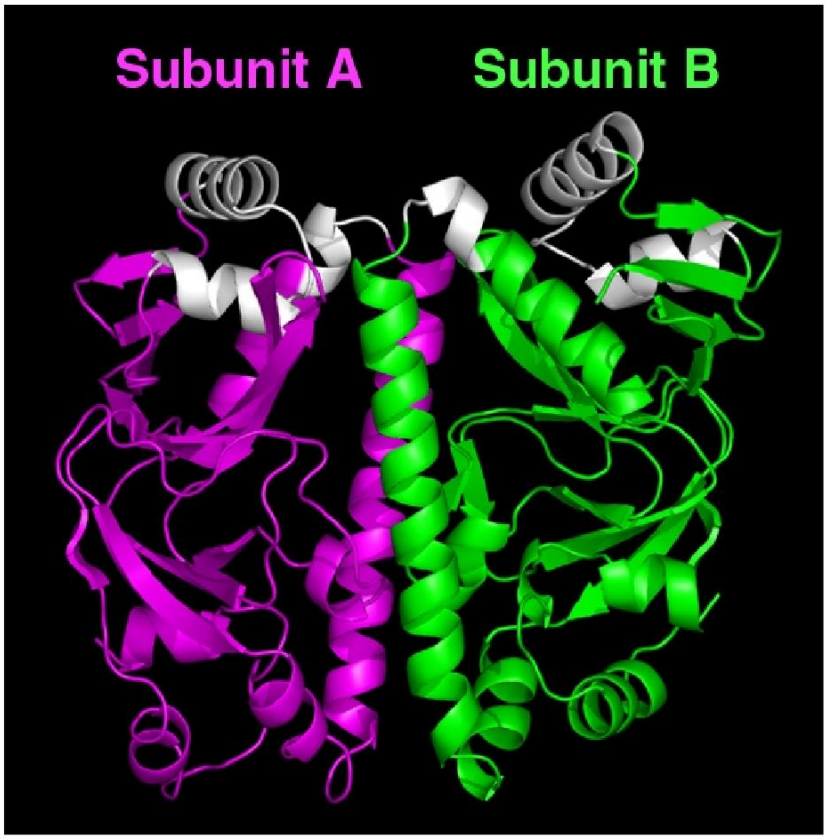

LEFT -- Ferritin molecule. RIGHT -- computer model of the defined structure for the "off" state of the cyclic AMP receptor protein found in mycobacterium tuberculosis. The two sub-units of the protein are genetically identical but asymmetric in shape in certain regions (Figure courtesy of Travis Gallagher, NIST).

Background -- Specular Neutron Reflectometry

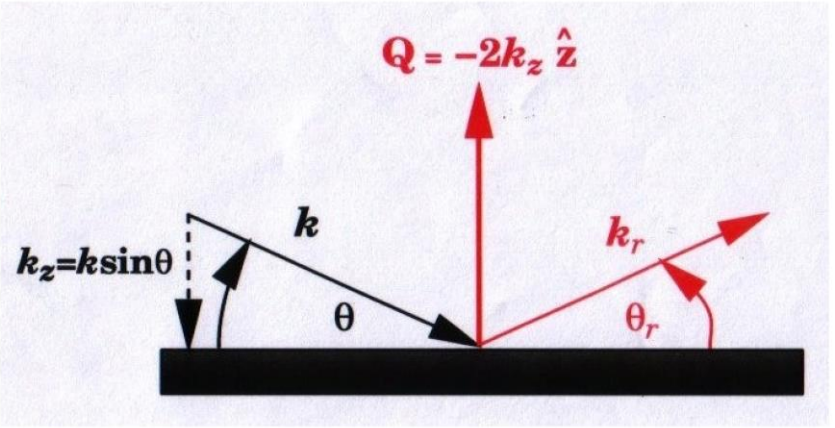

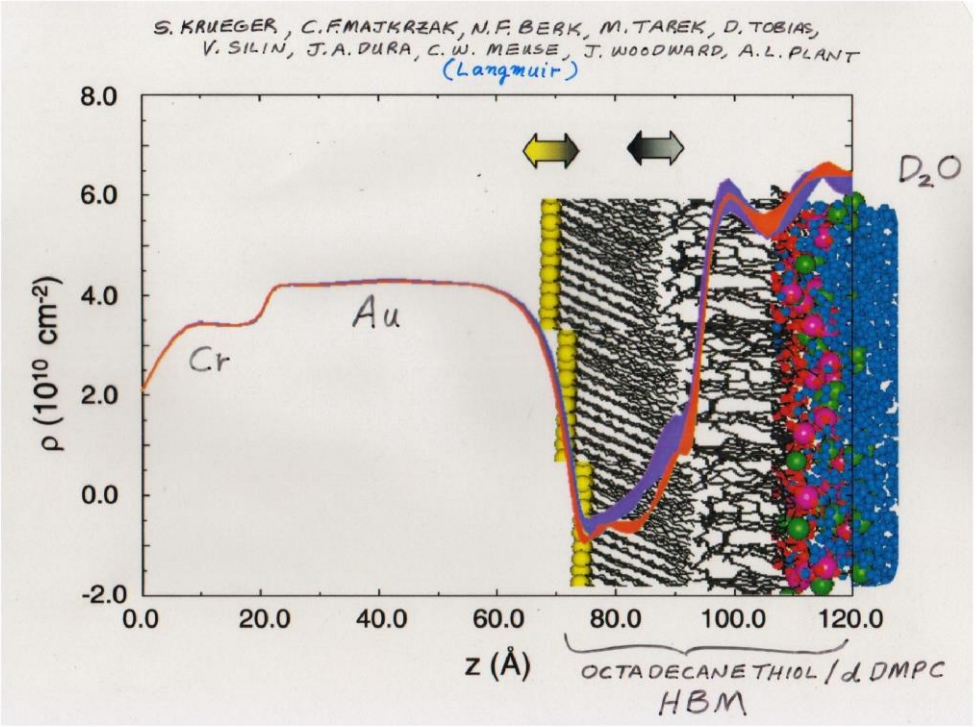

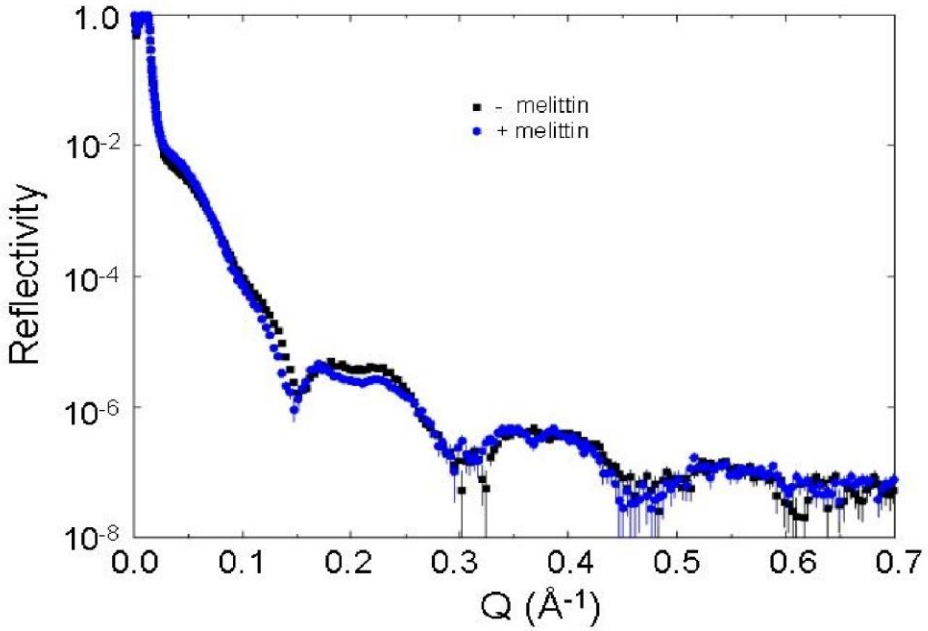
1.0
10-2
10-4
10-6
10-8
Reflectivity
- melittin
+ melittin
0.0
0.1
0.2
0.3
0.4
0.5
0.6
0.7
Q (Å-1)

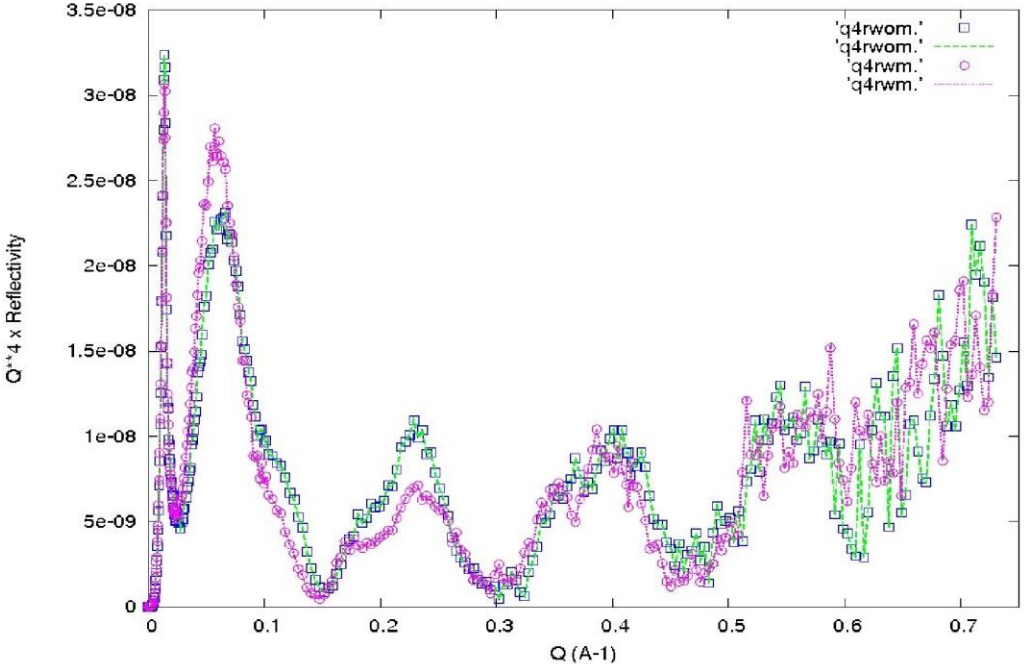
3.5e-08
3e-08
2.5e-08
2e-08
1.5e-08
1e-08
5e-09
0
Q**4 x Reflectivity
'q4rwom.'
'q4rwom.'
'q4rwm.'
'q4rwm.'
0
0.1
0.2
0.3
0.4
0.5
0.6
0.7
Q (A-1)

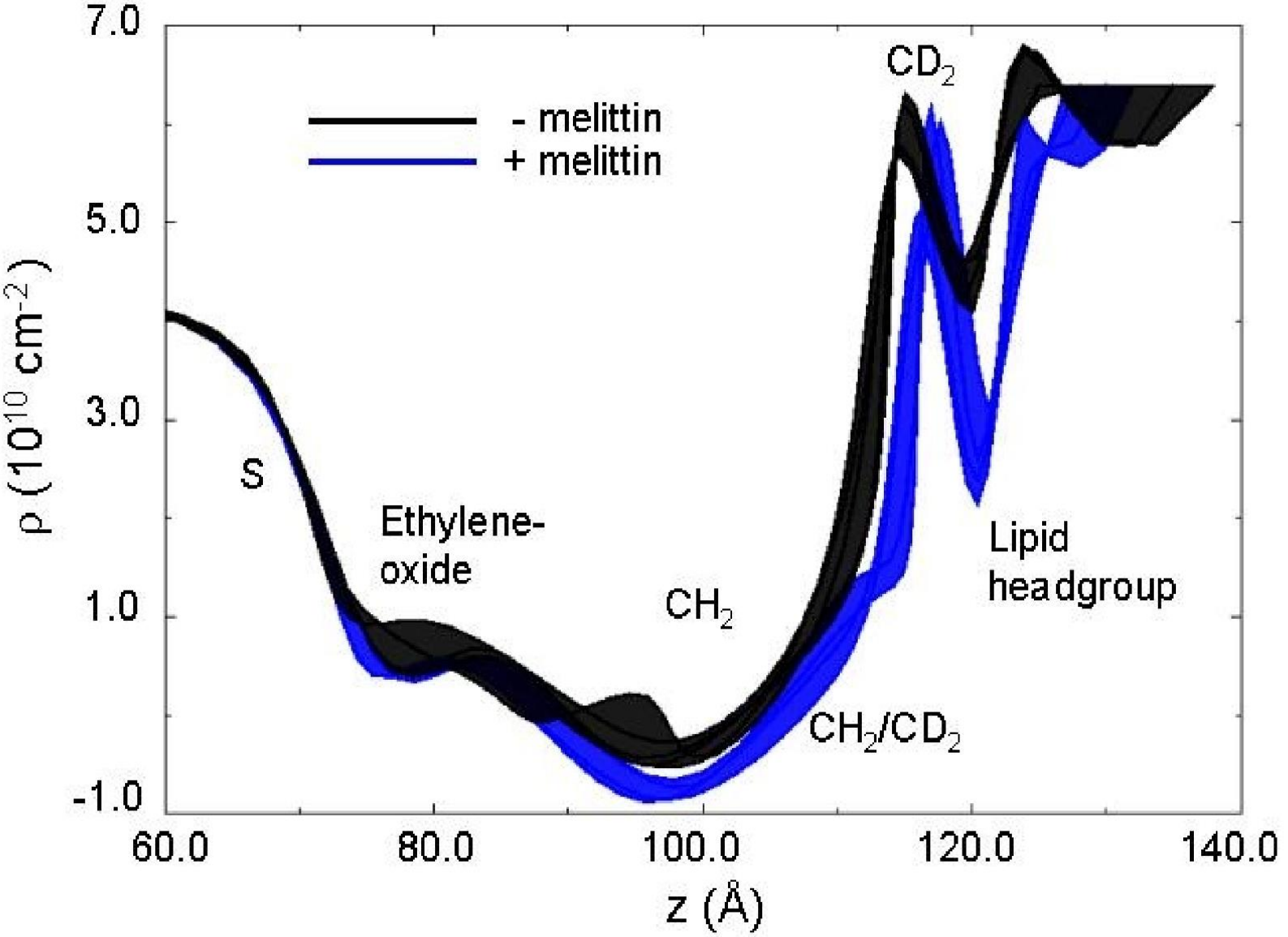
7.0
5.0
3.0
1.0
-1.0
ρ (10^10 cm^-2)
60.0
80.0
100.0
120.0
140.0
z (Å)
- melittin
+ melittin
CD2
S
Ethylene-
oxide
CH2
CH2/CD2
Lipid
headgroup

NEUTRON REFLECTION FROM A FLAT SURFACE

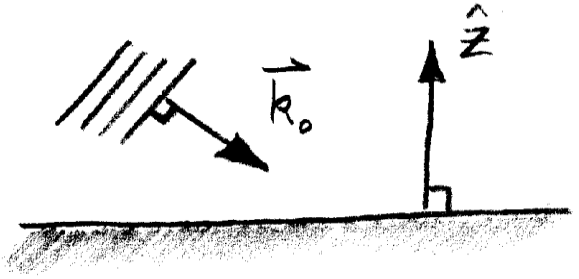

$$\Psi \propto e^{i\vec{k}\cdot\vec{r}}$$

$$\left[\frac{-\hbar^2}{2m}\nabla^2 + V(\vec{r})\right]\Psi = E\Psi$$

CONSERVATION OF ENERGY $\Rightarrow$

$$k^2 = k_0^2 - 4\pi\rho$$

SO $\left[\nabla^2 + k^2\right]\Psi = 0$ $\qquad \left(\eta^2 \equiv 1 - \frac{4\pi\rho}{k_0^2}\right)$

FOR SPECULAR REFLECTION,

$\vec{Q}\ (= \vec{k}_F - \vec{k}_I) \perp$ SURFACE

$$\left[\frac{\partial^2}{\partial z^2} + k_z^2\right]\Psi(z) = 0$$

$$k_z^2 = k_{0z}^2 - 4\pi\rho(z)$$

$$r(Q) = \frac{4\pi}{iQ} \int_{-\infty}^{+\infty} \psi(z)\, \rho(z)\, e^{i k_{0z} z}\, dz$$

$(Q = Q_z,\ \hat{z} \perp \text{SURFACE})$

& $\rho(z)$ IS THE IN-PLANE AVERAGE SLD

$$|r|^2 = \frac{I_R}{I_0}$$

$$r_{BA}(Q) \simeq \frac{4\pi}{iQ} \int_{-\infty}^{+\infty} \rho(z)\, e^{iQz}\, dz$$

The specular reflectivity is typically measured to an accuracy of 1 % on an absolute scale, normalized to the incident beam intensity. It is a highly quantitative probe from which real space structural depth profiles can be obtained with sub-nanometer resolution -- despite thin film sample volumes of the order of a millionth of a cubic centimeter.

PROBLEM: BORN APPROXIMATION FAILS AT SUFFICIENTLY SMALL Q — MUST THEN USE EXACT THEORY

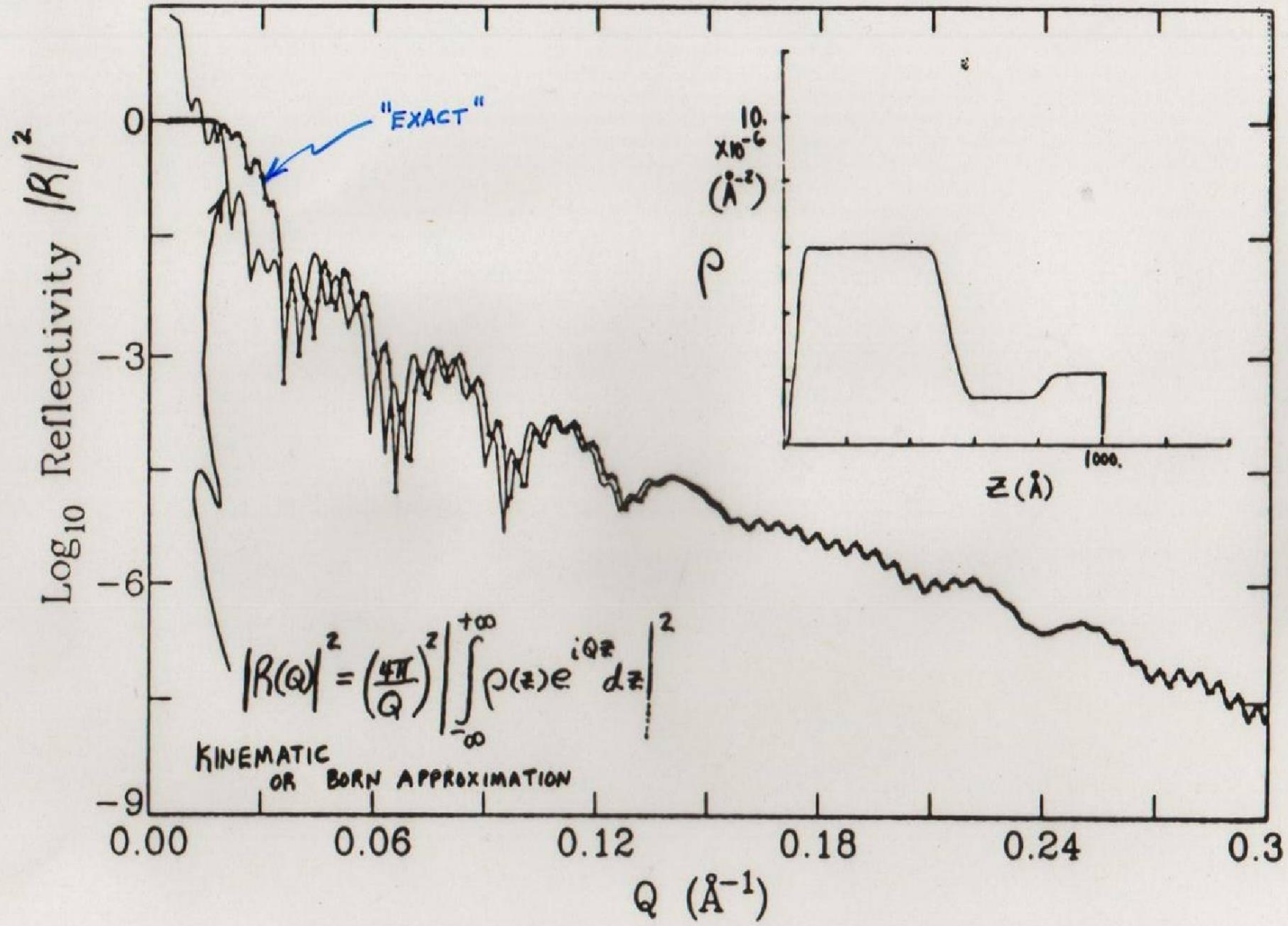

Comparison between kinematic (line) and dynamic (triangle + line) plus-state reflectivities for a density profile similar to that of Fig.2 as described in the text.

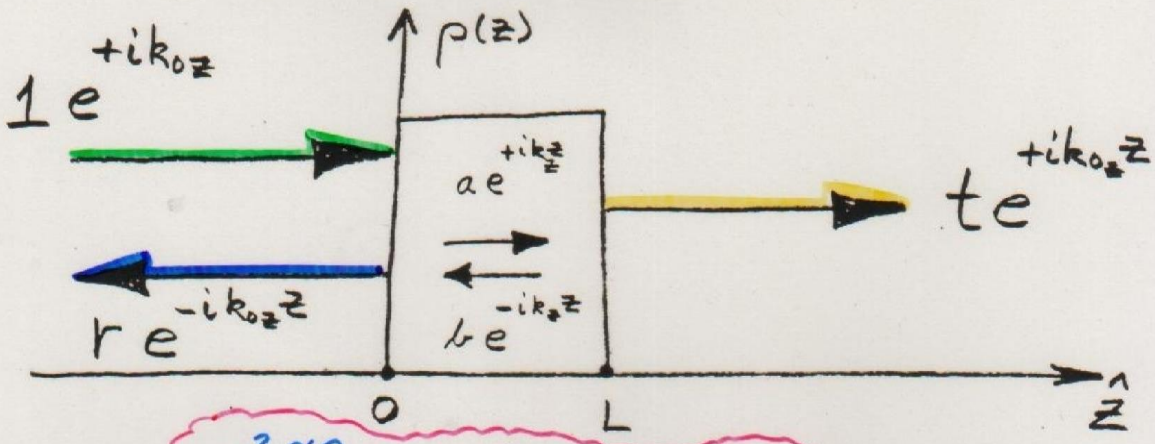

$$\frac{\partial^2 \psi(z)}{\partial z^2} + k_z^2 \psi(z) = 0$$

CONSERVATION OF MOMENTUM AND PARTICLE NUMBER REQUIRE THAT $\frac{\partial \psi(z)}{\partial z}$ AND $\psi(z)$ BE CONTINUOUS AT THE BOUNDARIES $z=0$ & $z=L$

$$\begin{pmatrix} t \\ it \end{pmatrix} e^{ik_{0z}L} = \begin{pmatrix} A & B \\ C & D \end{pmatrix} \begin{pmatrix} 1+r \\ i(1-r) \end{pmatrix}$$

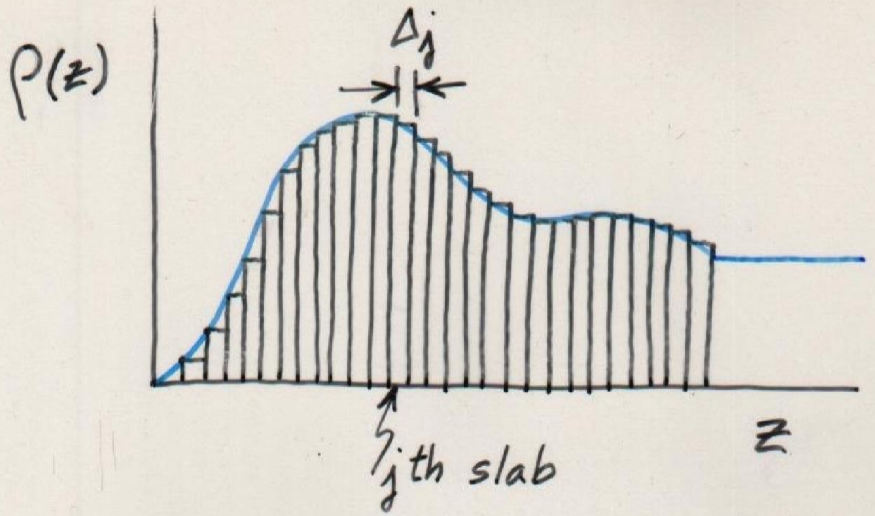

$$\begin{pmatrix} A & B \\ C & D \end{pmatrix} = \begin{pmatrix} a_N & b_N \\ c_N & d_N \end{pmatrix} \begin{pmatrix} a_{N-1} & b_{N-1} \\ c_{N-1} & d_{N-1} \end{pmatrix} \cdots \begin{pmatrix} a_2 & b_2 \\ c_2 & d_2 \end{pmatrix} \begin{pmatrix} a_1 & b_1 \\ c_1 & d_1 \end{pmatrix}$$

$$\begin{pmatrix} a_j & b_j \\ c_j & d_j \end{pmatrix} = \begin{pmatrix} \cos\delta_j & \frac{1}{n_{z_j}} \sin\delta_j \\ -n_{z_j} \sin\delta_j & \cos\delta_j \end{pmatrix}$$

$$\delta_j = k_{0z}\, n_{z_j}\, \Delta_j$$

$$= k_{z_j}\, \Delta_j$$

$z=L$ $\qquad\qquad$ $z=0$

$$\begin{pmatrix} 1 \\ \mathrm{i} \end{pmatrix} t(k)\mathrm{e}^{\mathrm{i}kL} = \begin{pmatrix} A_k(L) & B_k(L) \\ C_k(L) & D_k(L) \end{pmatrix} \begin{pmatrix} 1+r(k) \\ \mathrm{i}[1-r(k)] \end{pmatrix}$$

$$r = \frac{B+C+\mathrm{i}(D-A)}{B-C+\mathrm{i}(D+A)}$$

$$t = \frac{2\mathrm{i}\mathrm{e}^{-\mathrm{i}kL}}{B-C+\mathrm{i}(D+A)}$$

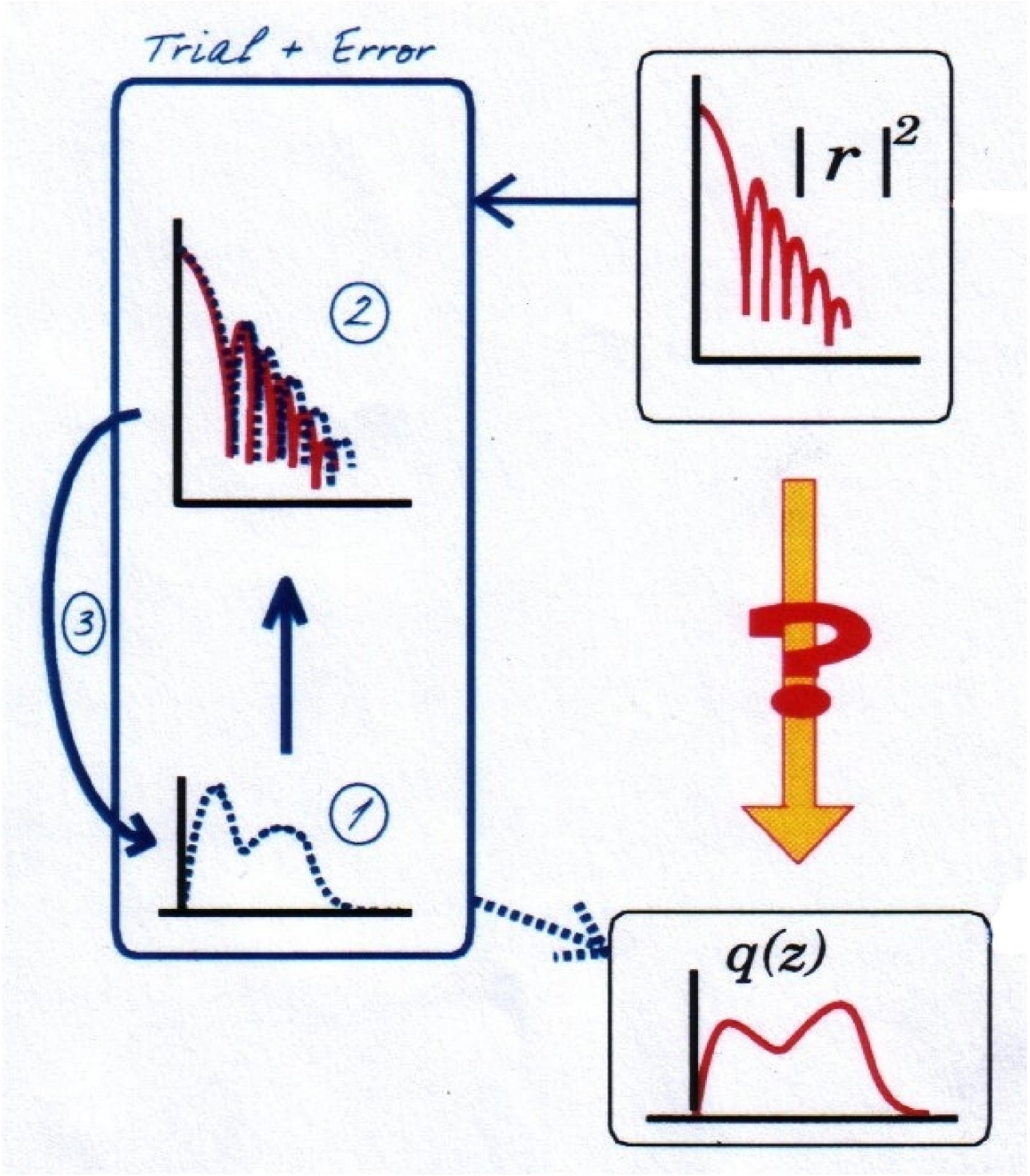
Trial + Error
$|r|^2$
2
3
1
?
$q(z)$

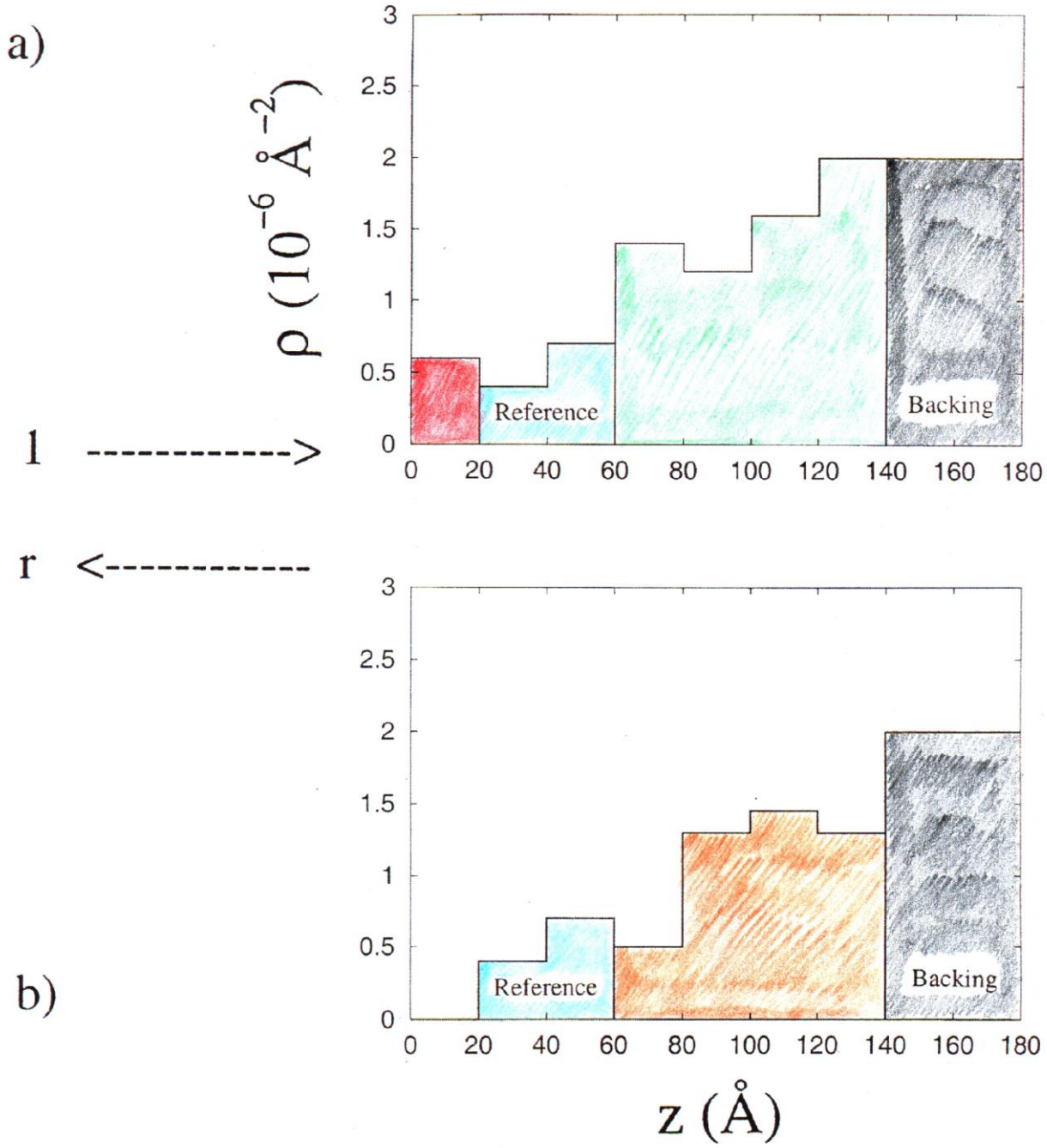
a)
ρ (10^-6 Å^-2)
3
2.5
2
1.5
1
0.5
0
Reference
Backing
0
20
40
60
80
100
120
140
160
180
l
r
b)
z (Å)

Figure 10.

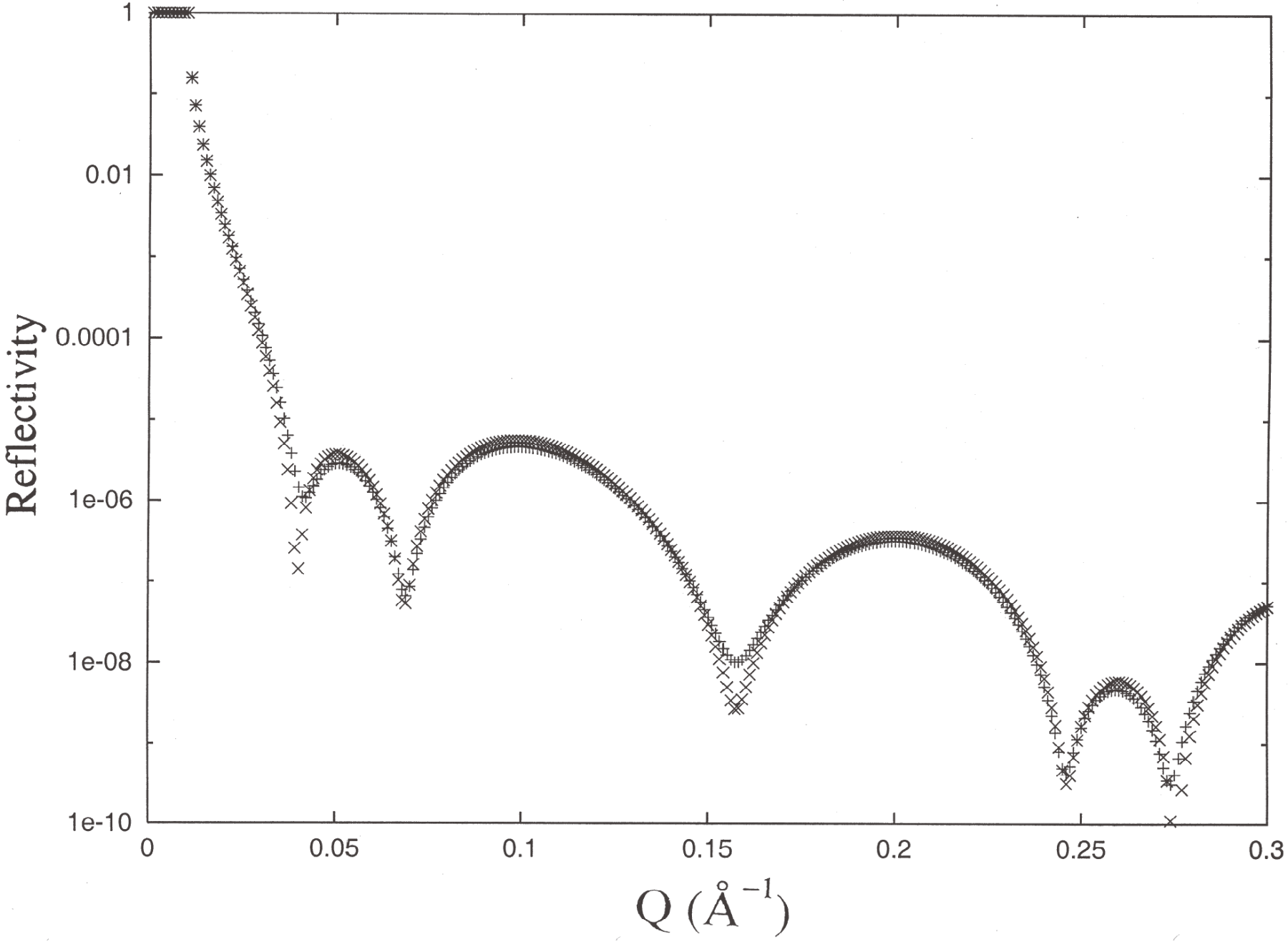
Reflectivity
1
0.01
0.0001
1e-06
1e-08
1e-10
0
0.05
0.1
0.15
0.2
0.25
0.3
Q (Å^{-1})

Figure 11.

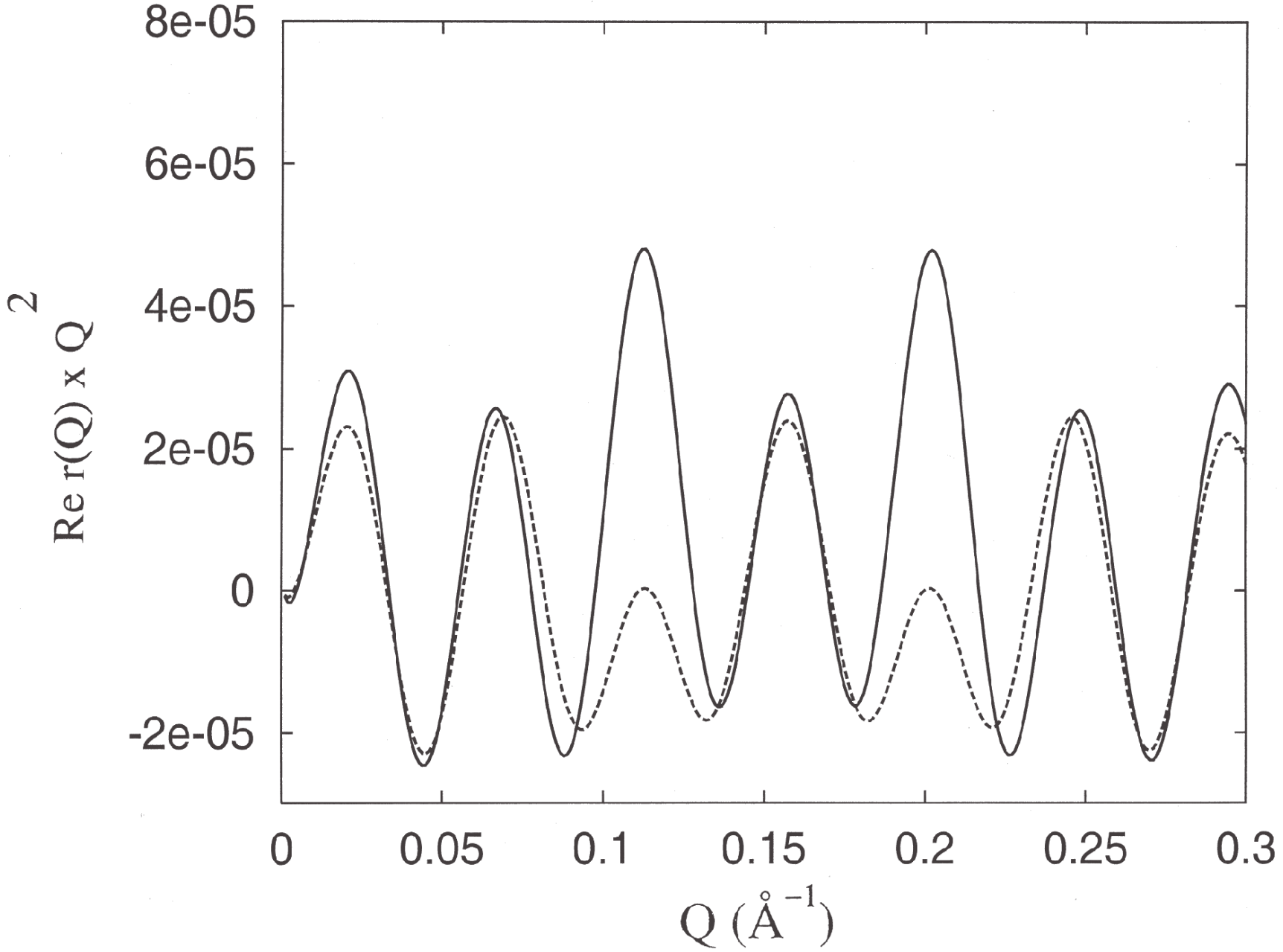

PBS

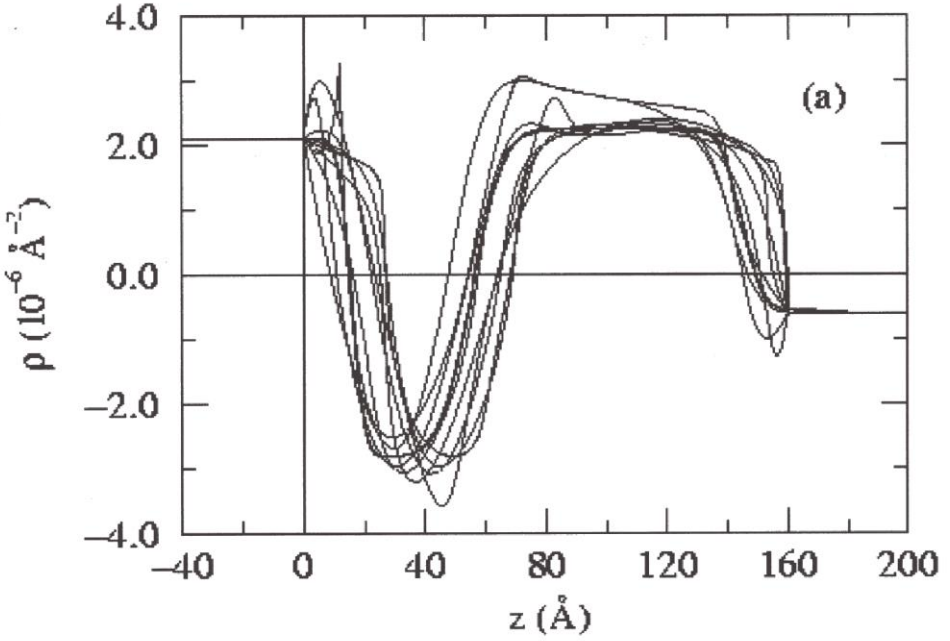
4.0
2.0
0.0
−2.0
−4.0
−40
0
40
80
120
160
200
(a)
ρ (10⁻⁶ Å⁻²)
z (Å)

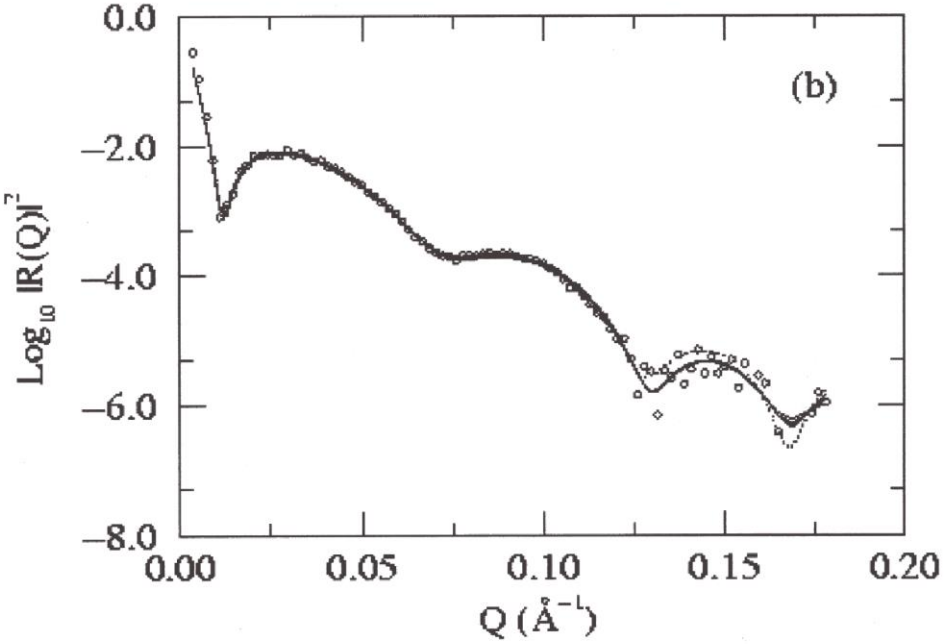
0.0
−2.0
−4.0
−6.0
−8.0
0.00
0.05
0.10
0.15
0.20
(b)
Log₁₀ |R(Q)|²
Q (Å⁻¹)

PBS

TiO in situ: Wiesler, et al.

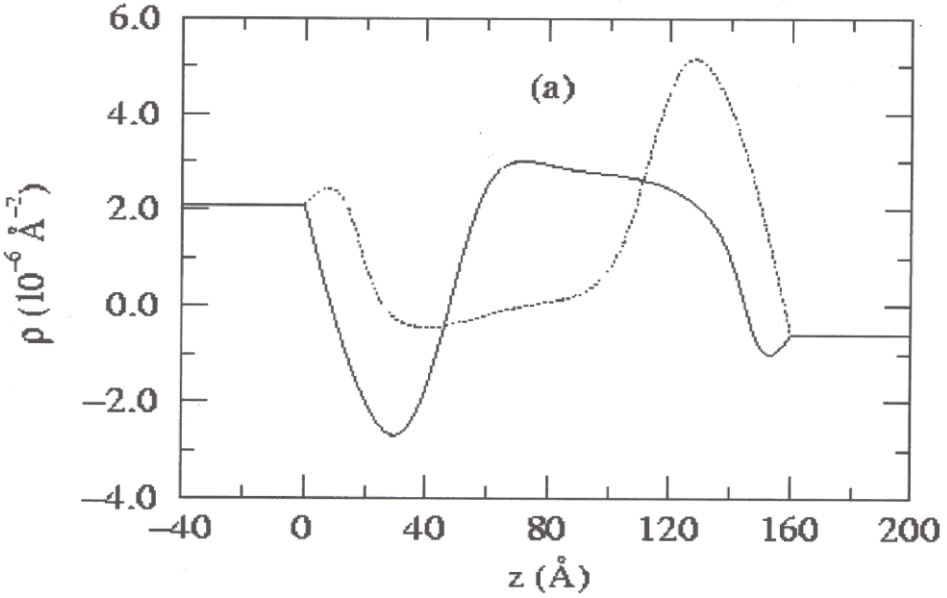

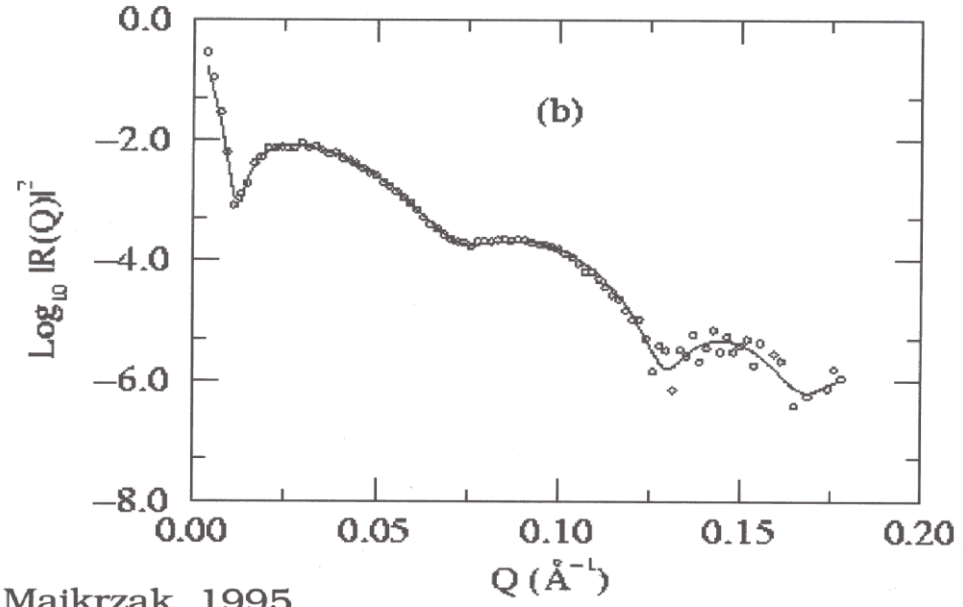

Berk & Majkrzak, 1995

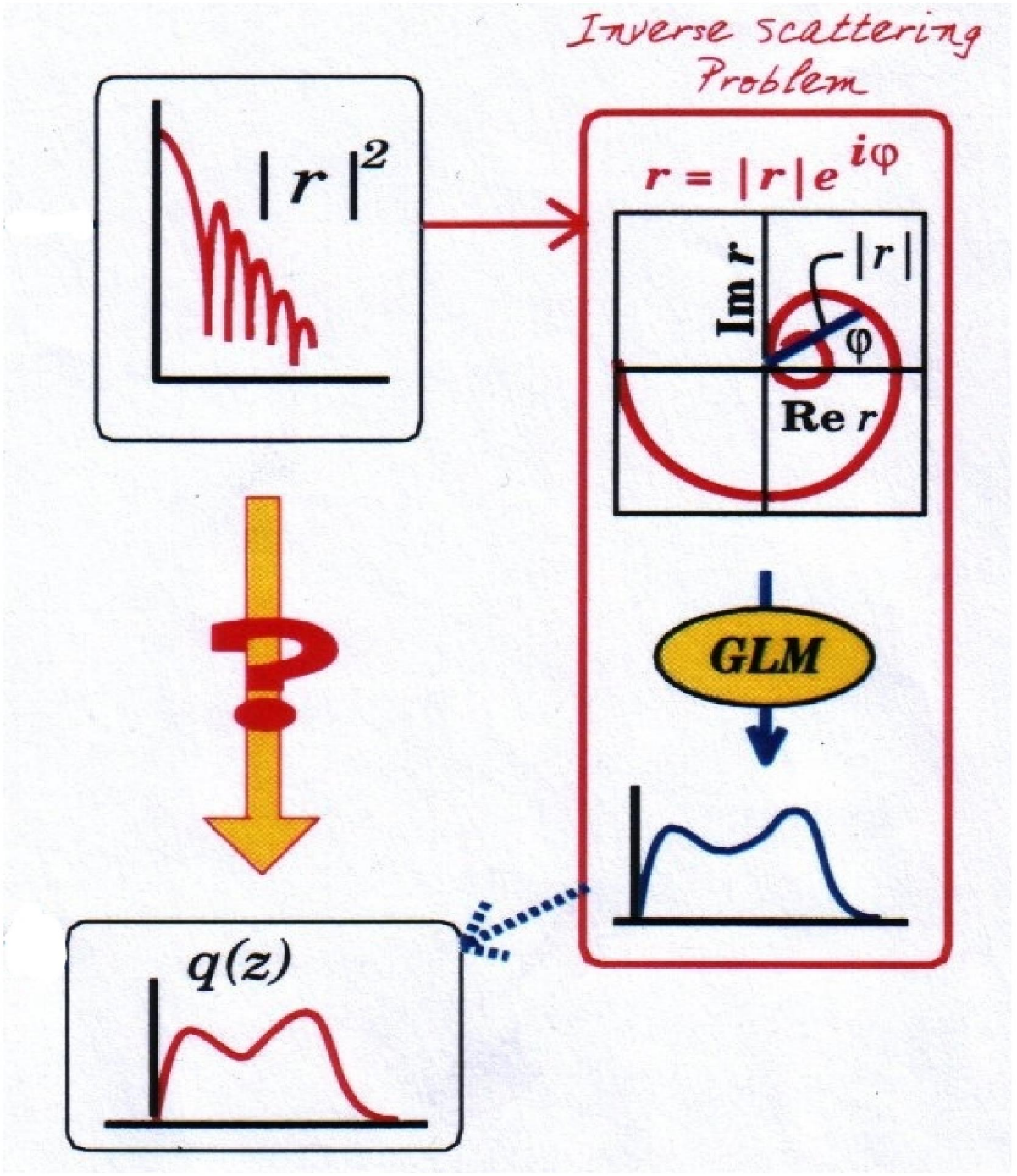
Inverse scattering Problem
$|r|^2$
$r = |r|e^{i\varphi}$
Im r
|r|
φ
Re r
GLM
q(z)

Phase Determination with 3 References

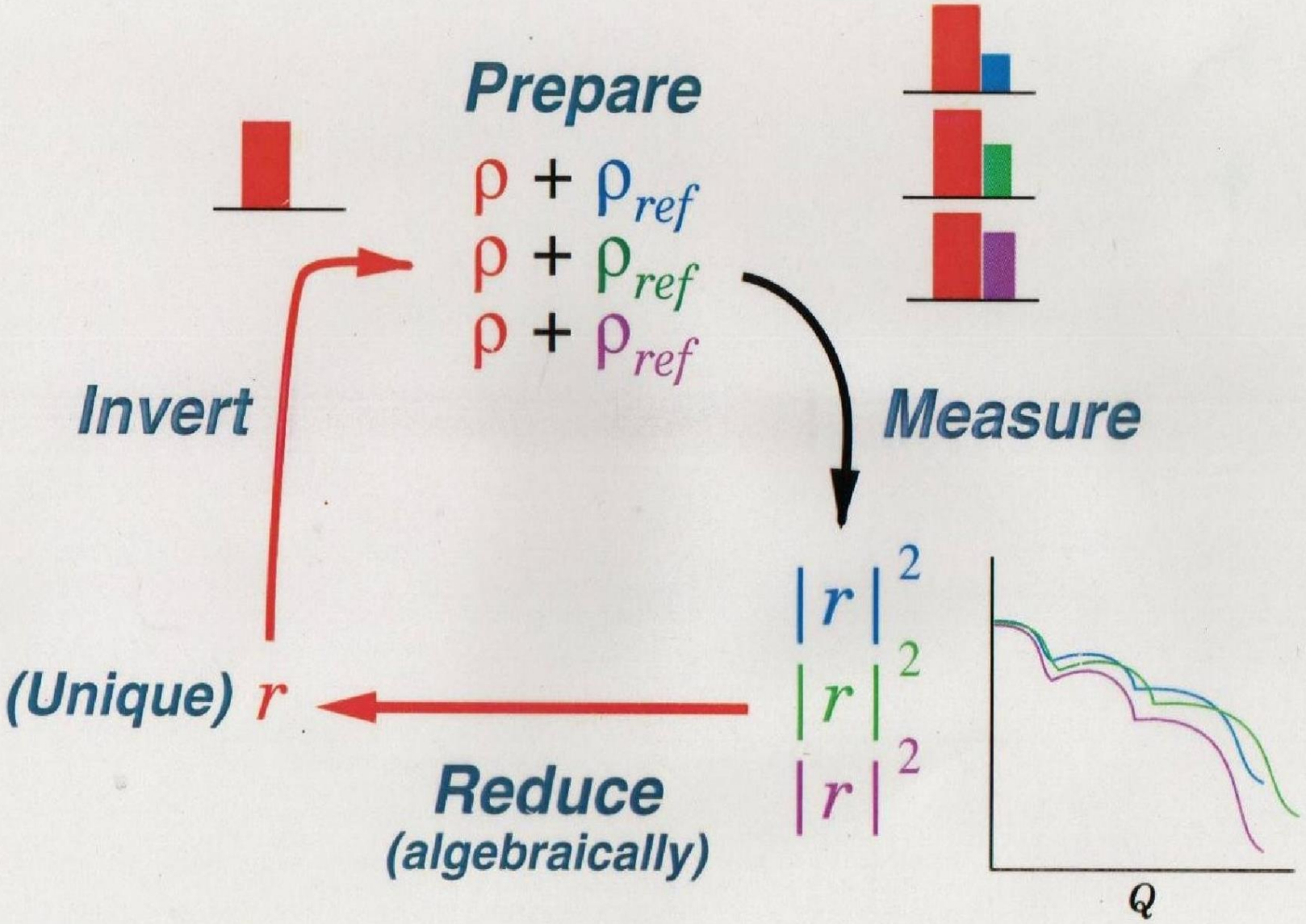

Majkrzak & Berk, 1995
de Haan, et al., 1995

FOURIER TRANSFORM OF THE COMPLEX REFLECTION AMPLITUDE

$$\mathcal{R}(z) = \frac{1}{\pi} \mathrm{Re} \int_0^\infty r(k_z) e^{i k_z z} \, dk_z$$

GEL'FAND LEVITAN MARCHENKO INTEGRAL EQUATION

$$K(z,\gamma) + \mathcal{R}(z+\gamma) + \int_{-z}^{+z} K(z,x) \mathcal{R}(x+\gamma) \, dx = 0$$

SCATTERING LENGTH DENSITY

$$\rho(z) = 2 \frac{d K(z,z)}{dz}$$

GIVEN THE COMPLEX REFLECTION AMPLITUDE, THE SCATTERING LENGTH DENSITY ρ CAN BE OBTAINED FROM AN EXACT, FIRST PRINCIPLE INVERSION FOR A REAL POTENTIAL OF FINITE EXTENT — AND THE SOLUTION IS UNIQUE!

NO FITTING, NO ADJUSTABLE PARAMETERS

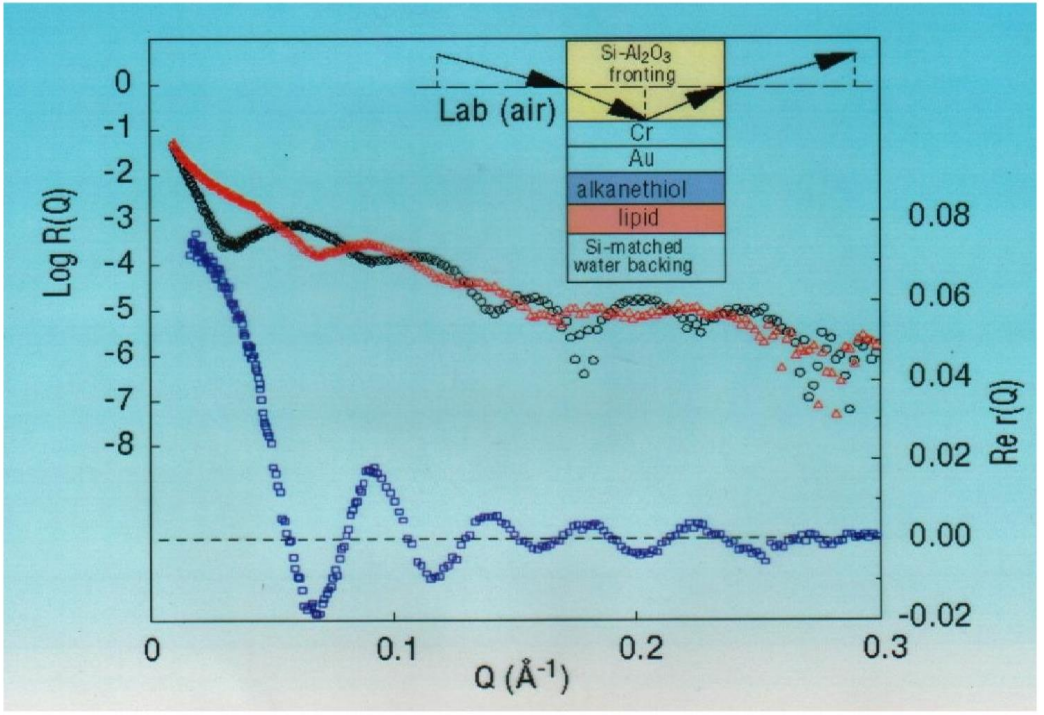
Si-Al2O3 fronting
Lab (air)
Cr
Au
alkanethiol
lipid
Si-matched water backing
Log R(Q)
Re r(Q)
Q (Å-1)
0
-1
-2
-3
-4
-5
-6
-7
-8
0.08
0.06
0.04
0.02
0.00
-0.02
0.1
0.2
0.3

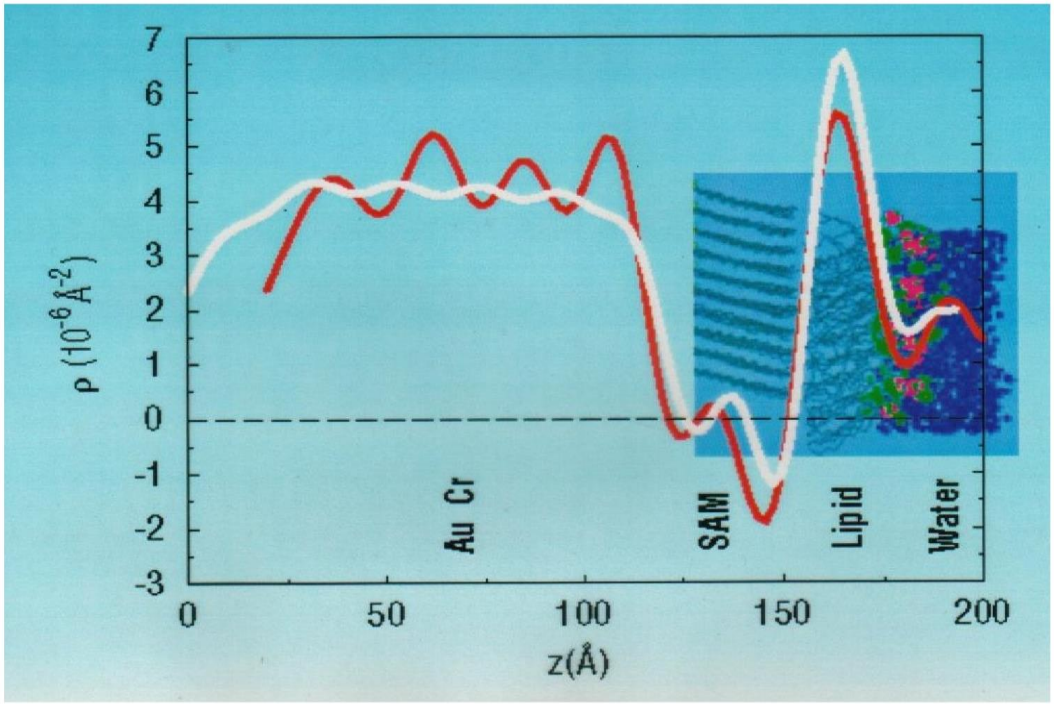
ρ (10-6Å-2)
z(Å)
Au Cr
SAM
Lipid
Water
7
6
5
4
3
2
1
0
-1
-2
-3
0
50
100
150
200

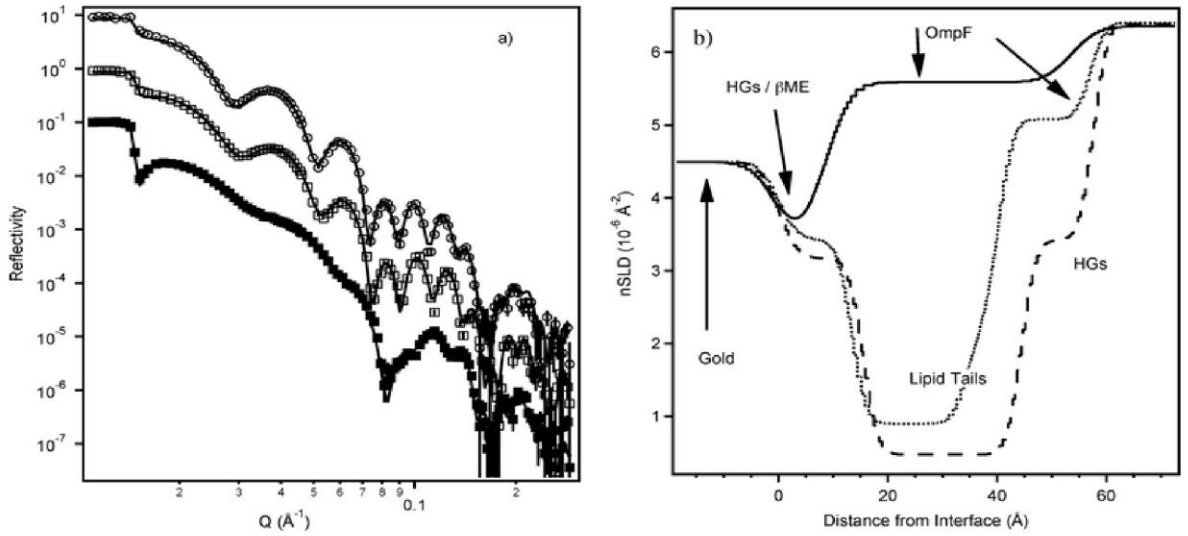

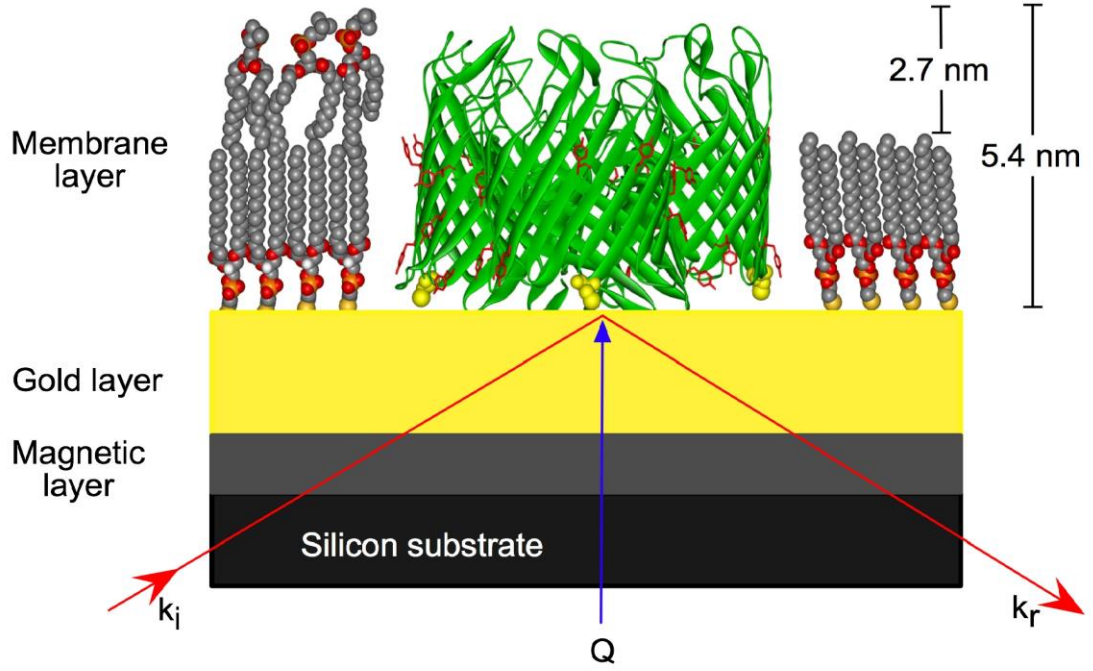

(Work of Anton Le Brun, Stephen Holt, and Jeremy Lakey et al.)

What's good about specular neutron reflectometry is that you can obtain, in principle (and in practice given data to high enough Q and of sufficiently low statistical uncertainty), a unique SLD profile along the surface normal with sub-nanometer spatial resolution (under proper conditions) for a protein/membrane system.

What's ***not so*** good about specular neutron reflectometry is that you can obtain, in principle (and in practice given data to high enough Q and of sufficiently low statistical uncertainty), a unique SLD profile ***only*** along the surface normal . . . .

Is it possible to apply methods used in phase-sensitive specular neutron reflectometry, an inherently one-dimensional spatial probe, to SANS in the dilute solution limit, an intrinsically three-dimensional investigative tool?

On the one hand, dilute solution SANS can be analyzed in a less-complicated theoretical framework due to the validity of the Born approximation while, on the other hand, the intrinsic orientational disorder has to be dealt with.

SANS IN THE DILUTE SOLUTION LIMIT FOR IDENTICAL MOLECULES

($\Longrightarrow$ NEGLIGIBLE COARELATION BETWEEN MOLECULES)

$$I_R(Q) \propto \left\langle \left| \int_{V_M} \rho(\vec{r})\, e^{i\vec{Q}\cdot\vec{r}}\, d^3r \right|^2 \right\rangle_\Omega$$

(BORN APPROXIMATION)

WHERE V_M IS THE VOLUME OF THE MOLECULE. USING

$$\left\langle e^{i\vec{Q}\cdot\vec{r}} \right\rangle_\Omega = \frac{\sin Qr}{Qr}$$

$$I_R(Q) \propto 4\pi \int_0^{D_{MAX}} r^2 \gamma(r) \frac{\sin Qr}{Qr}\, dr$$

WHERE $$\gamma(r) = \left\langle \int \Delta\rho(\vec{u})\Delta\rho(\vec{u}+\vec{r})\, d\vec{u} \right\rangle_\Omega$$

IS THE SPHERICALLY AVERAGED AUTOCORRELATION FUNCTION ($\Delta\rho \equiv \rho_M - \rho_0$ WHERE "M" $\Rightarrow$ MOLECULE & "0" $\Rightarrow$ SURROUNDING MEDIUM).

THE DISTANCE DISTRIBUTION FUNCTION $p(r) = r^2\gamma(r)$ AND REPRESENTS THE PROBABILITY THAT ANY TWO POINTS WITHIN THE MOLECULE ARE A DISTANCE r APART

$$\int_{V_M} \rho(\vec{r})\, e^{i\vec{Q}\cdot\vec{r}}\, d^3r$$ { STRUCTURE FACTOR

$$\underbrace{\rho_M \int_{V_M} e^{i\vec{Q}\cdot\vec{r}}\, d^3r}_{\text{FORM FACTOR (OR SHAPE)}}$$

FOR A MOLECULE OF UNIFORM SLD ρ_M

IN THE GUINIER LOW-Q APPROXIMATION,

$$I_R(Q) \simeq I_R(0)\, e^{-\frac{1}{3}Q^2R_G^2}$$

WHERE THE RADIUS OF GYRATION

$$R_G = \frac{\int_0^{D_{MAX}} r^2 p(r)\, dr}{2\int_0^{D_{MAX}} p(r)\, dr}$$

AND THE DISTANCE DISTRIBUTION FUNCTION

$$p(r) = \frac{r^2}{2\pi^2}\int_0^{\infty} Q^2 I_R(Q)\frac{\sin Qr}{Qr}\, dQ$$

Phase-sensitive small angle neutron scattering

C.F. Majkrzak[a], K. Krycka[a], S. Krueger[a], N.F. Berk[a,b], P. Kienzle[a], and B. Maranville[a]

[a]Center for Neutron Scattering, National Institute of Standards and Technology, Gaithersburg, MD
[b]Department of Materials Science and Engineering, University of Maryland, College Park, MD

[Published in *Journal of Applied Crystallography* **47** (2014) 780-787.]

Abstract

A method is described for determining the neutron scattering length density distribution of a molecular-scale object directly from phase-sensitive small angle neutron scattering (SANS). The structure factor amplitude is obtained through the use of a reference structure for a collection of randomly oriented, identical objects in the dilute solution limit (negligible inter-particle correlations). This work extends some of the techniques developed in recent years for phase-sensitive, specular neutron reflectometry to SANS, although the approach presented here is applicable only within the range of validity of the Born approximation. The scattering object is treated as a composite consisting of an "unknown" part of interest plus a reference component, the real-space structure of the latter being completely known. If, for example, the reference part of the object is composed of a ferromagnetic material (the magnetization of which is saturated), then polarized neutron beams can be employed to extract the information required for an unambiguous inversion of the scattering data without chemical substitution. The angular averaging over all possible relative orientations of the composite object does not result in a cancellation of the phase information since the reference and unknown parts of each object have a fixed spatial relationship. The new approach proposed here is not simply another type of isomorphic substitution, but also involves a reformulation of the underlying mathematical analysis of this particular scattering problem.

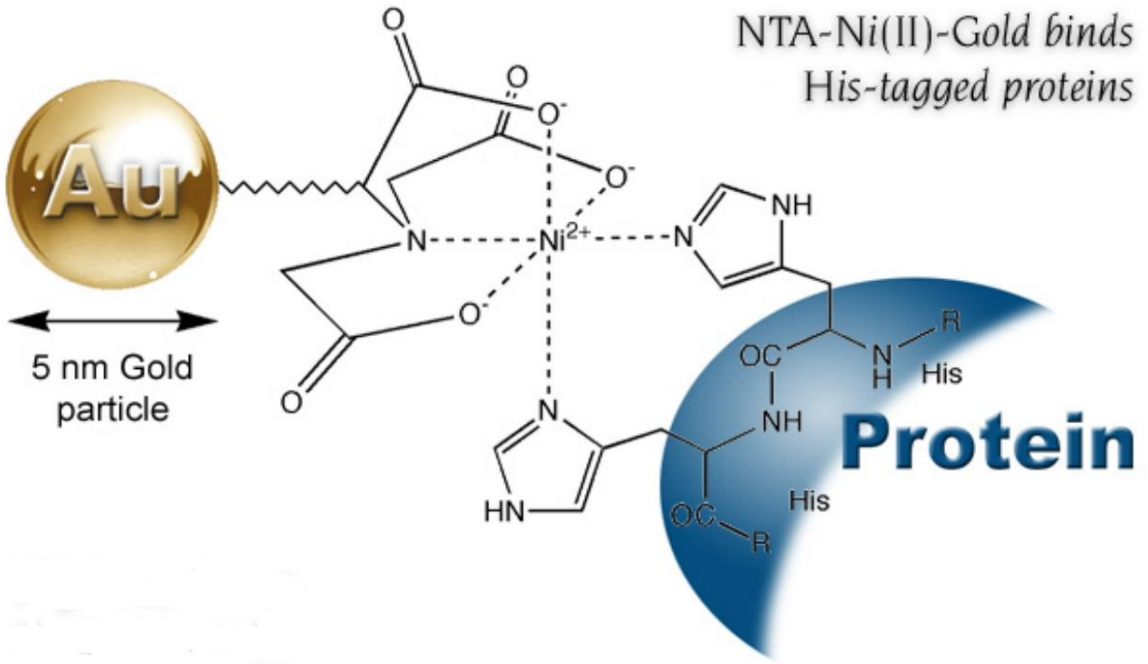

(http://www.nanoprobes.com/products/Ni-NTA-Na... Ni-NTA-Nanogold: His-tag labeling)

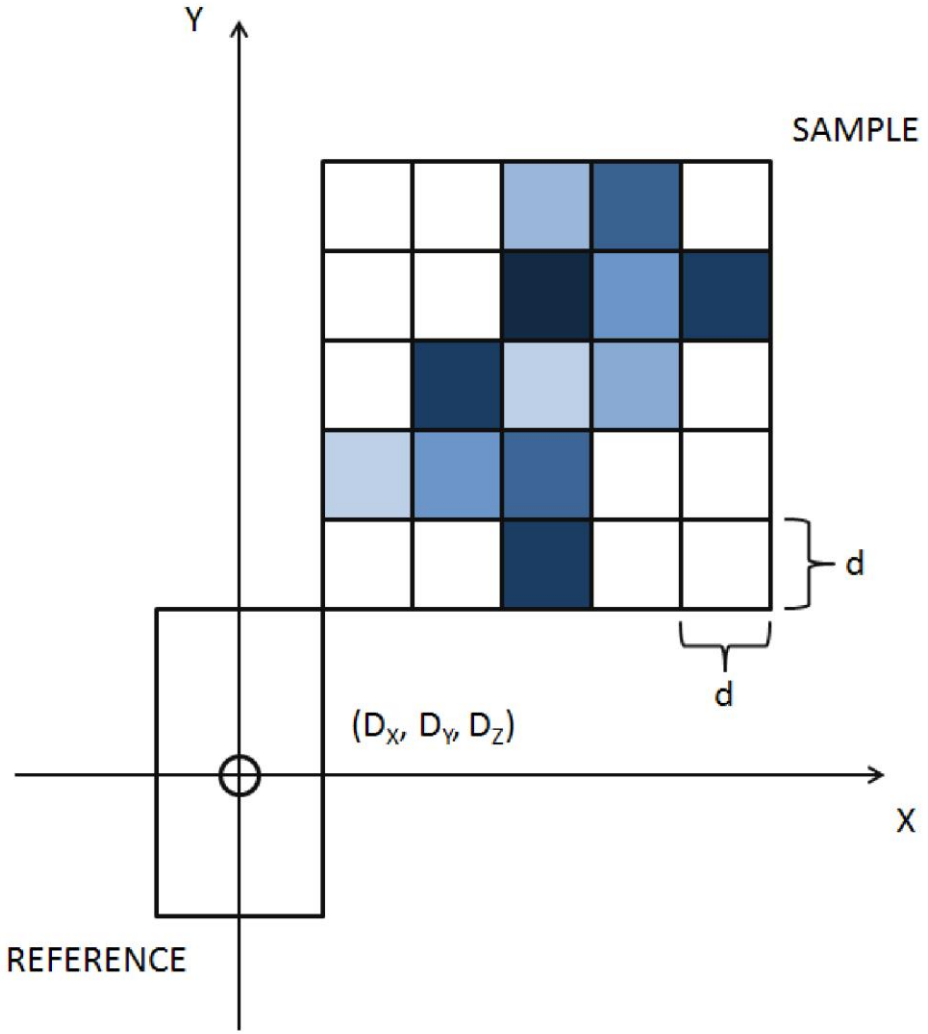

Figure 1. Diagram of a composite object (only a two-dimensional cut perpendicular to the z-axis is shown) consisting of some arbitrary component of interest, the structure of which is of unknown shape and scattering length density distribution, and an adjacent (and attached) reference part which is completely characterized. For clarity of exposition, it is assumed, without loss of generality, that the reference part is a simple rectangular solid of uniform SLD and centered on the origin of the reference frame fixed to the composite object. Thus, the reference part of the composite object is symmetric in this coordinate system. (The dimensions of the reference part are $2D_x$ x $2D_y$ x $2D_z$.) The other component, which can be of any shape and SLD distribution, is divided into sub-units of equal cubic volume d^3. This coordinate system is fixed with respect to the object.

Composite system = reference part + "unknown" part

(1) $F_C(\mathbf{Q}) = \iiint_{zyx} \rho(\mathbf{r})\, e^{iQ\cdot r}\, d\mathbf{r} = \iiint_{zyx} \rho(x,y,z)\, \exp[i(Q_x x + Q_y y + Q_z z)]\, dxdydz$

(2) $$F_C(\mathbf{Q}) = F_R(\mathbf{Q}) + F_S(\mathbf{Q})$$

(3) $$|F_C|^2 = |F_R|^2 + |F_S|^2 + 2\mathrm{Re}F_R\, \mathrm{Re}F_S$$

since F_R is real for a symmetric reference.

Orientational averaging

(4) $$< |F_C|^2 > = < |F_R|^2 > + < |F_S|^2 > + < 2ReF_R\ ReF_S >$$

(5) $$D(Q) \equiv < |F_{CA}|^2 > - < |F_{CB}|^2 > = < |F_{RA}|^2 > - < |F_{RB}|^2 > + 2U(Q)$$

where $$U(Q) = < ReF_{RA}\ ReF_S > - < ReF_{RB}\ ReF_S >$$

(6) $$U(Q) = (1/2)\ [_{MEAS}D(Q) - (_{CALC}< |F_{RA}|^2 > - _{CALC}< |F_{RB}|^2 >)]$$

$$= [< ReF_{RA}\ ReF_S > - < ReF_{RB}\ ReF_S >]$$

Structure factor for reference

$$(7) \quad F_R = \iiint_{zyx} \rho_R \, e^{i\mathbf{Q}\cdot\mathbf{r}} \, d\mathbf{r} = \iiint_{zyx} \rho_R \exp[i(Q_x x + Q_y y + Q_z z)] \, dxdydz$$

$$= \rho_R \iiint_{zyx} \exp[iQ_x x] \exp[iQ_y y] \exp[iQ_z z] \, dxdydz$$

$$= [8\rho_R / (Q_x Q_y Q_z)] \sin(Q_x D_x) \sin(Q_y D_y) \sin(Q_z D_z) = \mathrm{Re}F_R$$

Structure factor for "unknown" sample part

$$(8) \quad F_S = \iiint_{zyx} \rho_S(x,y,z) \exp[iQ_x x] \exp[iQ_y y] \exp[iQ_z z] \, dxdydz$$

Consider, for example, an expansion of the integration along the x-direction in Equation (8):

$$\int_x \rho_S(x,y,z) \exp[iQ_x x] \, dx$$

$$= \rho_{S1}(y,z) \int_{Dx}^{Dx+d} \exp[iQ_x x] \, dx + \rho_{S2}(y,z) \int_{Dx+d}^{Dx+2d} \exp[iQ_x x] \, dx + \cdots$$

$$+ \rho_{Sl}(y,z) \int_{Dx+(l-1)d}^{Dx+ld} \exp[iQ_x x] \, dx + \rho_{SL}(y,z) \int_{Dx+(L-1)d}^{Dx+Ld} \exp[iQ_x x] \, dx$$

$$= \sum_{l=1}^{L} \rho_{Sl}(y,z) \, (2/Q_x) \exp\{iQ_x[D_x + (d/2)(2l-1)]\} \sin(Q_x d/2)$$

After doing similarly along the y- and z-directions, we obtain

(9) $$ReF_S = [8/(Q_xQ_yQ_z)] \sin(Q_xd/2) \sin(Q_yd/2) \sin(Q_zd/2) \bullet$$

$$\sum_{l=1}^{L} \sum_{m=1}^{M} \sum_{n=1}^{N} {}_S\rho_{lmn} \cos\{Q_x[D_x - (d/2) + ld] + Q_y[D_y - (d/2) + md] + Q_z[D_z - (d/2) + nd]\}$$

where d is the edge of a sub-unit cube of the sample part of the object's volume which is rendered into L x M x N such sub-units, each one having an individual but constant SLD, ${}_S\rho_{lmn}$, corresponding to the (l,m,n) th sub-unit.

Interference term

Using Equations (6), (7), and (9), we can now write the function U(Q) explicitly as

$$(10)\quad U(Q) = \langle ReF_{RA}\, ReF_S \rangle - \langle ReF_{RB}\, ReF_S \rangle = \langle ReF_{RA}\, ReF_S - ReF_{RB}\, ReF_S \rangle$$

$$= \langle [ReF_{RA} - ReF_{RB}]\, ReF_S \rangle$$

$$= \langle [8/(Q_xQ_yQ_z)]^2 (\rho_{RA} - \rho_{RB}) \sin(Q_xD_x)\sin(Q_yD_y)\sin(Q_zD_z) \bullet$$

$$\sin(Q_xd/2)\sin(Q_yd/2)\sin(Q_zd/2) \bullet$$

$$\sum_{l=1}^{L} \sum_{m=1}^{M} \sum_{n=1}^{N} {}_S\rho_{lmn} \cos\{Q_x[D_x - (d/2) + ld] + Q_y[D_y - (d/2) + md] +$$

$$Q_z[D_z - (d/2) + nd]\} \rangle$$

or $$\mathbf{U(Q) = \sum_{l=1}^{L} \sum_{m=1}^{M} \sum_{n=1}^{N} {}_S\rho_{lmn} \langle C_{lmn}(Q_x, Q_y, Q_z) \rangle}$$

Coefficients

(11) $< C_{lmn} (Q_x , Q_y , Q_z) > = < [8/(Q_x Q_y Q_z)]^2 (\rho_{RA} - \rho_{RB}) \bullet$

$\sin(Q_x D_x)\sin(Q_y D_y)\sin(Q_z D_z) \bullet$

$\sin(Q_x d/2)\sin(Q_y d/2)\sin(Q_z d/2) \bullet$

$\cos\{Q_x[D_x - (d/2) + ld] + Q_y[D_y - (d/2) + md] + Q_z[D_z - (d/2) + nd]\}>$

where the orientational averaging is defined (Andrews, 2004) as

(12) $< C_{lmn} (Q_x , Q_y , Q_z) > = [1/(8\pi^2)] \iiint_{\alpha\beta\gamma} C_{lmn} (\alpha, \beta, \gamma) \sin\beta \, d\beta \, d\alpha \, d\gamma$

in which the integration limits for the angles α, β, and γ are zero to 2π, π, and 2π, respectively, and the rectangular components of **Q**, (Q_x , Q_y , Q_z), in the object coordinate system are expressed in terms of the angles of integration by

(13) $Q_x = Q (\cos\gamma \cos\alpha - \cos\beta \sin\alpha \sin\gamma)$

$Q_y = Q (- \sin\gamma \cos\alpha - \cos\beta \sin\alpha \cos\gamma)$

$Q_z = Q (\sin\beta \sin\alpha)$

$Q = |\mathbf{Q}| = (Q_x^2 + Q_y^2 + Q_z^2)^{1/2} = [4\pi \sin(SA/2)] / \lambda$

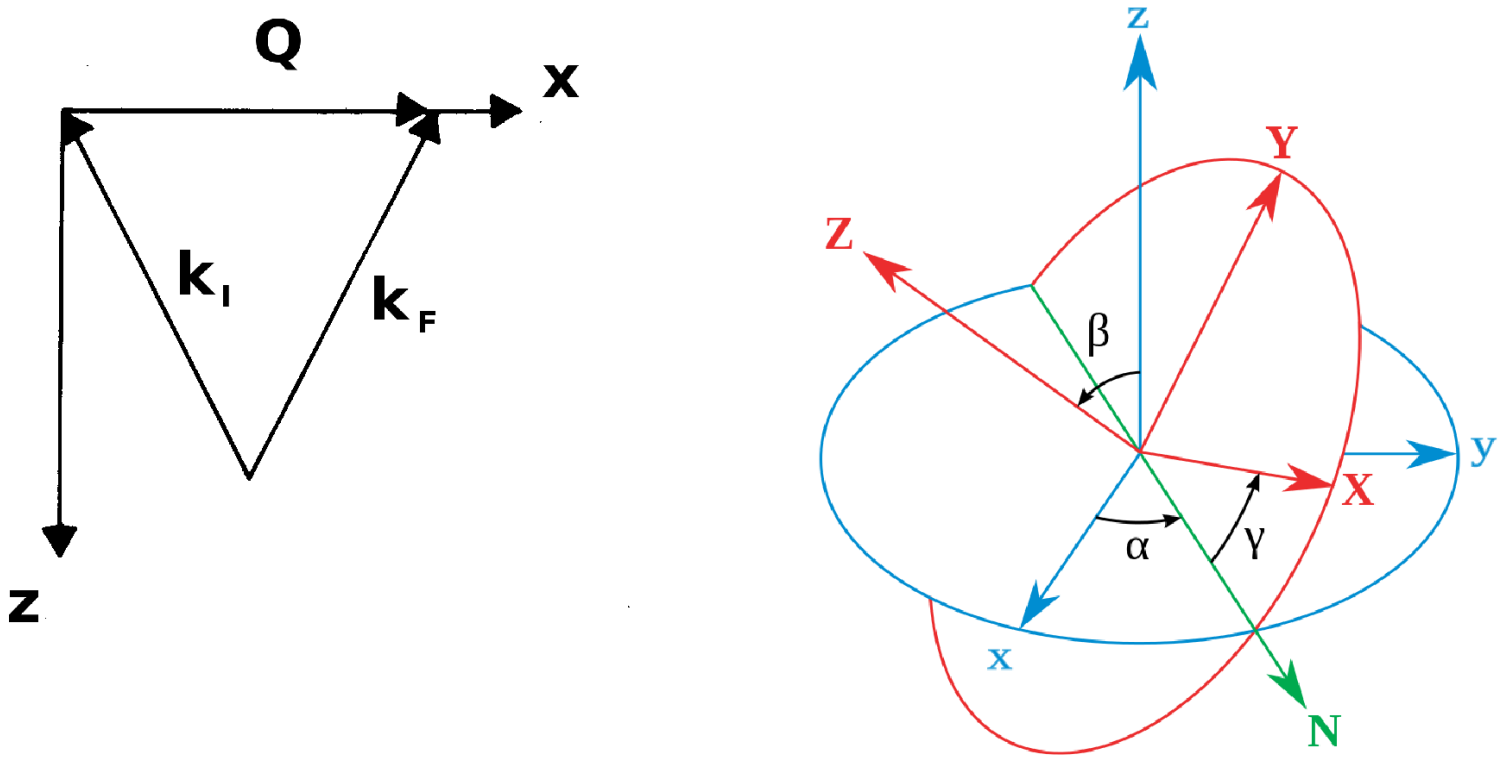

Figure 2. The schematic (on the right) illustrates the relationship between axes of the object and laboratory in terms of the Euler angles (Goldstein, 1980). The diagram on the left shows the scattering geometry in the laboratory frame of reference for one plane of a continuum rotated about the incident beam direction (along the nominal $\mathbf{k}_I$). ($\mathbf{Q} = \mathbf{k}_F - \mathbf{k}_I$.) (Right part of figure courtesy of L. Brits, Wikipedia.)

Saturated ferromagnetic reference

One possible reference choice for SANS, if a polarized incident beam and polarization analysis of the reflected beam is available, is a ferromagnetic material, either saturated in a remanent state along a specific direction in the reference frame fixed to each object or along a single direction in the laboratory frame of reference as defined by the application of an external magnetic field. For a non-magnetic sample part of the object, the selection rules for polarized neutron scattering (Moon et al., 1969) are such that only non-spin-flip (NSF) scattering processes convey structural information about it. If neutrons are incident in the "+" state (one of two possible spin eigen-states), then the reflected beam will also be in that same polarization state -- and analogously for an incident beam in the "-" state. Taking the neutron polarization axis to be along the Z-direction in the laboratory frame of reference, the two corresponding expressions for the SLDs for a polarized neutron beam are given by

$$\rho = \rho_N \pm \rho_M q_{HVZ} \tag{14}$$

where ρ_N and ρ_M correspond to the nuclear and magnetic SLDs, respectively, + / - indicates the neutron spin state, and q_{HVZ} is the Z-component of the Halperin vector (Moon et al., 1969) which determines the extent of the coupling between the neutron spin and the atomic magnetic moments of the material through the relationship

$$q_{HVZ} = \cos \varphi_{QZ} \cos \varphi_{QS} - \cos \varphi_{SZ} \tag{15}$$

where φ_{QZ} is the angle between **Q** and the neutron polarization direction (as already specified to be the laboratory Z-axis), φ_{QS} is the angle between **Q** and the atomic spin (opposite to its associated magnetic moment), and φ_{SZ} is the angle between the atomic spin and the laboratory Z-axis.

For the specific case where the neutron polarization **P** is along the laboratory Z-axis (which is perpendicular to **Q** , which in turn has been taken to lie along the laboratory X-axis) and each object's ferromagnetic magnetization points along the laboratory Z-axis as well (by application of an applied external magnetic field), then $q_{HVZ} = +1$ so that

(16) $$\rho = \rho_N \pm \rho_M$$

The nuclear and magnetic contributions to the overall SLD of the reference part effectively add or subtract depending on the spin state of the incident neutron. (In practice, it is simpler to maintain the neutron polarization axis along the incident beam direction $\mathbf{k}_I$, but the correction for this case is small compared to that for which **P** is always arranged to be exactly perpendicular to **Q** -- and the difference has negligible consequences for the simpler example we have chosen to illustrate.) Two references are thereby achieved without any physical change to the composite object and all that is required is to collect two scattered intensity data sets, one for neutron spin plus and the other for spin minus incident, to obtain U(Q). Note that in this particular case, the magnetic reference in conjunction with polarized neutron beam measurements is essentially equivalent to an isotopic exchange of material with a different nuclear SLD in the reference part.

Alternatively, if the neutron polarization **P** is still along the laboratory Z-axis (again, perpendicular to **Q** which is along the laboratory X-axis) but the magnetization of each object is always directed along the negative z-axis of the coordinate system fixed in the same orientation to each object (in a remanent state), then ρ is given by

$$\rho = \rho_N \pm \rho_M \cos\beta \tag{17}$$

where cos β is simply the direction cosine between a given object's z-axis and the Z-axis of the laboratory reference system.

Non-magnetic reference

Although the use of polarized neutrons and saturated ferromagnetic references attached to the sample of interest may have certain distinct advantages, there are other reference possibilities. Suppose, for instance, that the sample object of interest can be chemically attached to a known molecular structure. Then, in analogy to Equation (4) we can write

$$(18) \qquad \langle |F_C|^2 \rangle = \langle |F_{KR}|^2 \rangle + \langle |F_{TBD}|^2 \rangle + \langle 2ReF_{KR}\, ReF_{TBD} \rangle$$

where it is assumed that the scattered intensity as a function of Q can be measured in separate experiments for: 1) the composite system (denoted by the subscript "C"); 2) the "known reference" part "KR" alone (taken to be symmetric and not yet attached to the unknown "to be determined" part "TBD"); and 3) the unknown part TBD by itself. Since all of the components on the RHS of Equation (18) can be measured independently ($\langle |F_{KR}|^2 \rangle$ could also be calculated, in principle) and ReF_{KR} can be calculated, then the SLDs associated with a finite element decomposition of TBD, the part of interest, can be determined in the same way as shown previously in the derivation culminating in Equation (10).

As long as the structure factor for the composite object can be expressed as a sum of separable terms, one for the sample part and the other corresponding to the reference component, then the method presented here is applicable. For example, it is possible to adopt a configuration in which the reference volume is contained within that of the sample component -- or, vice versa -- assuming that the structure and material composition of the reference part is completely known in either case.

The choice of reference is not completely arbitrary, however. The symmetry of the reference part can be important. For example, consider a simple two-dimensional square sample object divided into four square sub-cells where the reference part is also taken to be square ($D_x = D_y$) with its sides parallel to those of the sample part of the composite object. Then the inversion of U(Q) can only yield SLD values for the two sample sub-cells lying along a diagonal perpendicular to the reference diagonal which runs from the origin out to the point (D_x , D_y) which are equal to their average. Optimization of the reference structure can be an important consideration.

2D model calculation

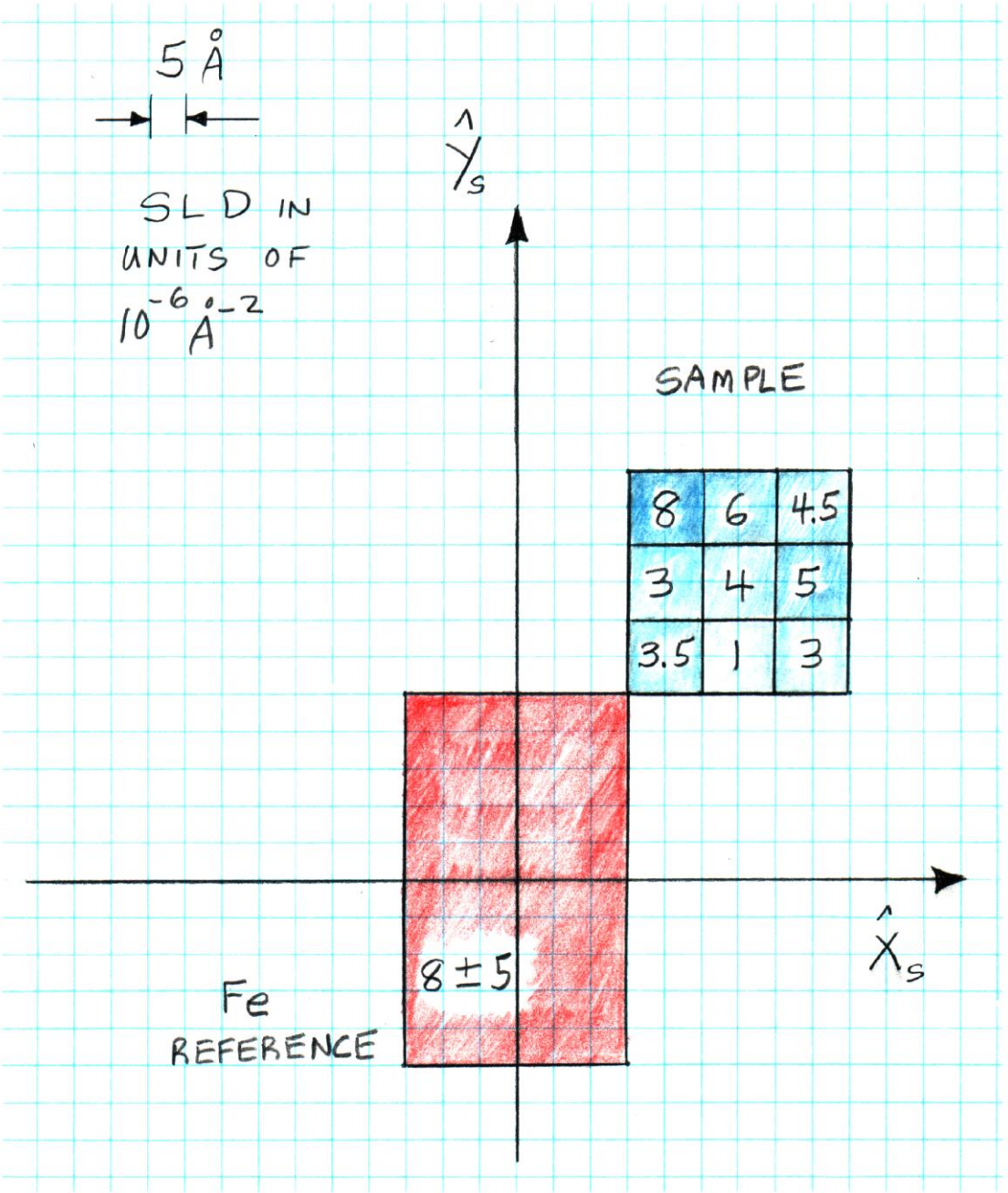

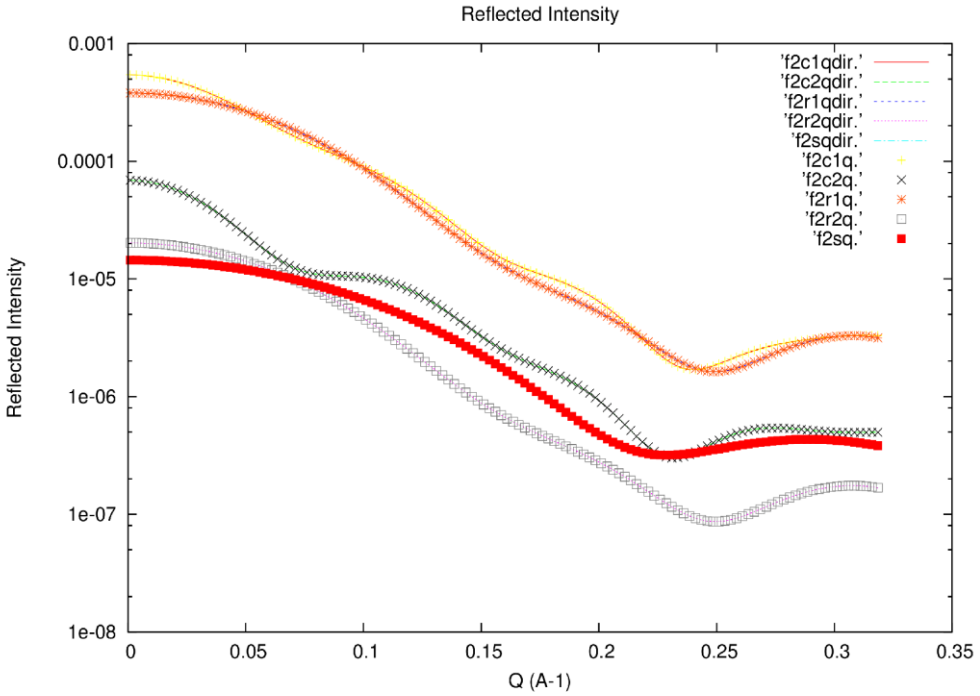
Reflected Intensity
Reflected Intensity
Q (A-1)
'f2c1qdir.'
'f2c2qdir.'
'f2r1qdir.'
'f2r2qdir.'
'f2sqdir.'
'f2c1q.'
'f2c2q.'
'f2r1q.'
'f2r2q.'
'f2sq.'
0.001
0.0001
1e-05
1e-06
1e-07
1e-08
0
0.05
0.1
0.15
0.2
0.25
0.3
0.35

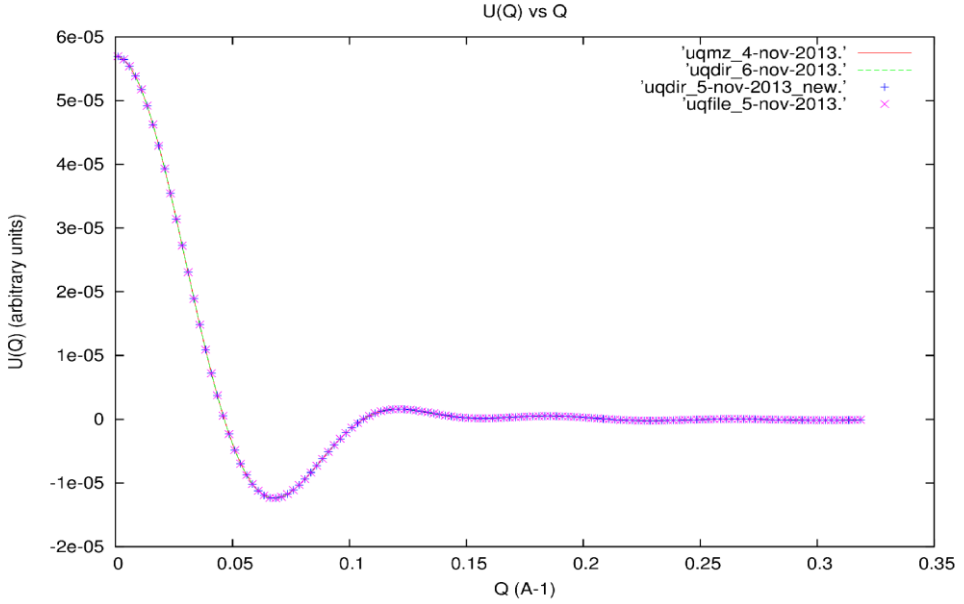
U(Q) vs Q
U(Q) (arbitrary units)
Q (A-1)
'uqmz_4-nov-2013.'
'uqdir_6-nov-2013.'
'uqdir_5-nov-2013_new.'
'uqfile_5-nov-2013.'
6e-05
5e-05
4e-05
3e-05
2e-05
1e-05
0
-1e-05
-2e-05
0
0.05
0.1
0.15
0.2
0.25
0.3
0.35

Results of inversion (by SVD)

1	3.499999999998708E-06
2	1.000000000002320E-06
3	2.999999999999607E-06
4	2.999999999999298E-06
5	3.999999999997135E-06
6	5.000000000001029E-06
7	8.000000000002012E-06
8	5.999999999997062E-06
9	4.500000000000755E-06

(SLD in A^-2)

Model calculation in 3D

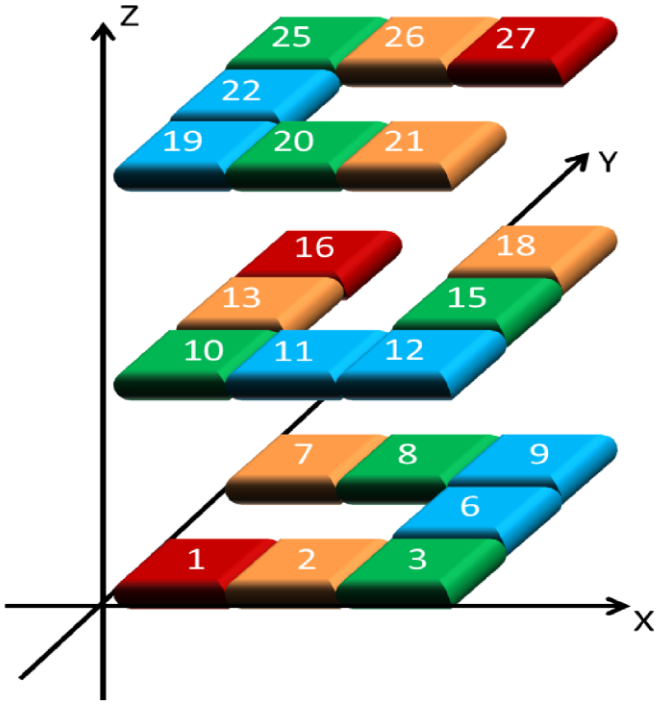

Figure 3. An exploded view (the layers are actually in contact with one another along the z-axis) of a model SLD distribution described within a volume containing 27 cubic sub-cells, each 10 Angstrom on a side. Adjacent to this sample object, a ferromagnetic reference consisting of a single rectangular block of dimensions (2 x 15 Å) x (2 x 25 Å) x (2 x 35 Å), along the x-, y-, and z-axes, respectively, is centered at the origin of the composite object reference system and has a uniform SLD. Advancing along the positive z-axis, there is a counter-clockwise chirality. The alternative index "j" of the (l,m,n) th sub-cell shown in the diagram is given by j = (n-1)NM + (m-1)M + l where the total number of sub-cells is L x M x N = 3 x 3 x 3 = 27. The SLDs of sub-cells 4, 5, 14, 17, 23 and 24 are zero.

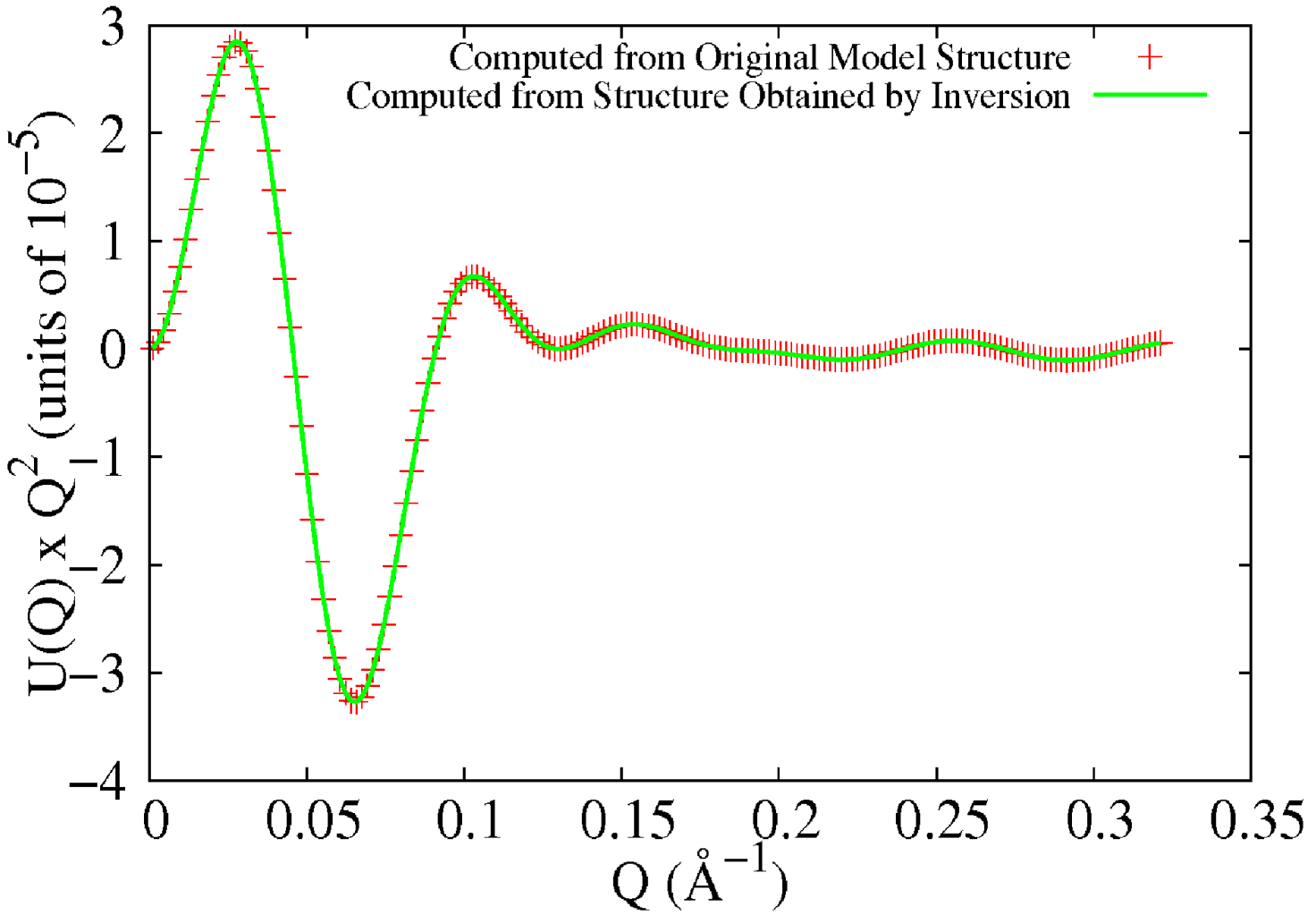

Figure 4. The scattering function U(Q) as calculated from the formulas derived in earlier sections using the model values of the sub-cell SLDs listed in Table 1 multiplied by Q^2 for clarity in the plot (+ symbols). The dashed line represents the function U(Q) as calculated for the SLD values obtained by inversion of the original U(Q) computed from the starting model SLD values. The SLD values obtained via inversion are also given in Table I.

Table I. Original model SLDs and the corresponding set obtained by inversion of U(Q).

Sub-cell index	Model SLD ($Å^{-2}$)	SLD via inversion of U(Q) ($Å^{-2}$)
1	8.0e-06	7.9952567492373344E-06
2	5.0e-06	5.1581725329032674E-06
3	3.0e-06	3.0569598364690891E-06
4	0.0	-7.2533473459990216E-08
5	0.0	-1.5660148421135301E-07
6	2.0e-06	2.2978778672140286E-06
7	5.0e-06	4.8739136996700097E-06
8	3.0e-06	2.9930326061456065E-06
9	2.0e-06	2.1984348123739998E-06
10	3.0e-06	2.9629299578242556E-06
11	2.0e-06	2.1925726598984072E-06
12	2.0e-06	1.6436400553807519E-06
13	5.0e-06	4.7519473764813062E-06
14	0.0	1.5486577358675494E-07
15	3.0e-06	3.1727620721836486E-06
16	8.0e-06	7.9598602881746376E-06
17	0.0	-6.9083620588432130E-07
18	5.0e-06	5.2662142595539992E-06
19	2.0e-06	2.2331881840833366E-06
20	3.0e-06	2.7336203622214004E-06
21	5.0e-06	4.9615602336763678E-06
22	2.0e-06	2.2545626421854936E-06
23	0.0	2.2333899747162826E-07
24	0.0	-5.4189888528353584E-08
25	3.0e-06	2.8814918203719384E-06
26	5.0e-06	5.0080273594332235E-06
27	8.0e-06	7.9993090554343 01E-06

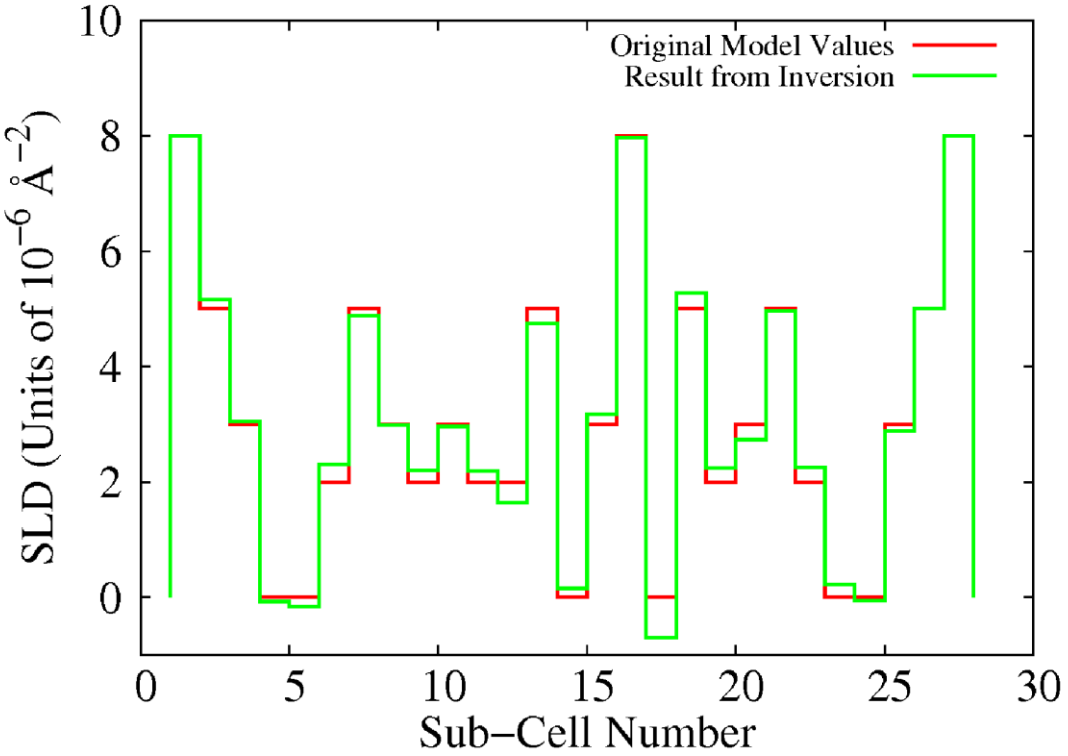

Figure 5. Histogram representation of the distribution of SLD values of the sample sub-cells as solved numerically by singular value decomposition (dashed line) compared to the original corresponding model values (solid line). The same information is contained in Table 1. The agreement between the SLD distribution obtained by inversion of the model generated scattering function U(Q) and that of the original model is remarkably good.

Conclusions

<> We have proposed a procedure to directly and unambiguously obtain the SLD distribution for a molecular structure via SANS through the use of reference structures attached to the object of interest. The proposed method is applicable for a collection of identical molecular-scale objects which are randomly oriented in angle in solution in the dilute concentration limit (where inter-particle correlations are negligible) where the Born approximation is valid. In particular, saturated ferromagnetic references in conjunction with polarized neutron beams make it possible, in principle, to employ a single form of the composite object.

<> The new method proposed here is not simply another type of isomorphic substitution, but also involves a reformulation of the underlying mathematical analysis of this particular scattering problem. Instead of extracting a radius of gyration or distance distribution function, a finite element approach in conjunction with a rearrangement of the structure factor expressions, including the angular averaging over all possible orientations of the sample object, allows for a direct and unambiguous determination of the SLD distribution. Numerical simulations of the technique presented here on model systems support these conclusions.

<> Given that the proposed method has been demonstrated in principle here, practical realization will require reference structures which can be used to create the necessary composite samples.

Appendix

IF ρ IS NOT EXACTLY $\rho(z)$,
i.e., SOME VARIATIONS EXIST IN
THE (x,y)- PLANE, THEN

$$r_{BORN} \simeq \frac{4\pi}{iQ} \int_{-\infty}^{+\infty} \langle \rho(x,y,z) \rangle_{x,y} \, e^{iQz} \, dz$$

ON SPECULAR "RIDGE" WHERE $\vec{Q} = Q_z \hat{z}$

WHERE

$$\langle \rho(x,y,z) \rangle_{x,y} = \frac{1}{A} \iint_{-\infty-\infty}^{+\infty+\infty} \rho(x,y,z) \, dx dy$$

$$= \bar{\rho}(z) \text{ ONLY}$$

& $\bar{A}$ = NORMALIZING AREA OF THE (X,Y)- PLANE

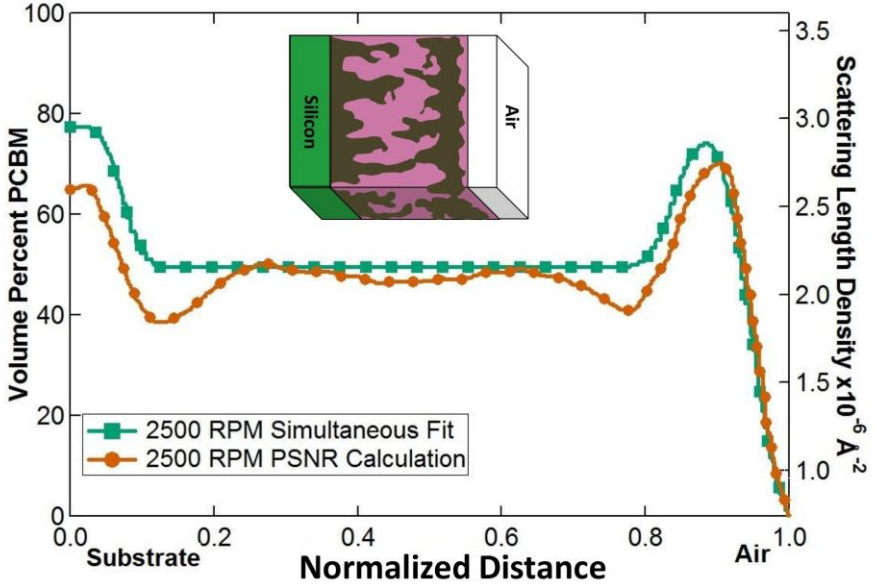
Volume Percent PCBM
Scattering Length Density x10^{-6} Å^{-2}
Normalized Distance
Substrate
Air
Silicon
Air
2500 RPM Simultaneous Fit
2500 RPM PSNR Calculation
0
20
40
60
80
100
1.0
1.5
2.0
2.5
3.0
3.5
0.0
0.2
0.4
0.6
0.8
1.0

FORMALISM ALLOWS A COMPOSITE POTENTIAL TO BE EXPRESSED AS A PRODUCT:

$$\underbrace{\begin{pmatrix} A & B \\ C & D \end{pmatrix}}_{\text{COMPOSITE (1,2,3)}} = \underbrace{\begin{pmatrix} a & b \\ c & d \end{pmatrix}}_{\text{UNKNOWN}} \underbrace{\begin{pmatrix} w & x \\ y & z \end{pmatrix}}_{\text{REFERENCE (1,2,3)}}$$

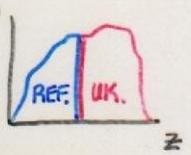

$$|R(Q)|^2 = |R_1(Q)|^2,\ |R_2(Q)|^2, \text{ and } |R_3(Q)|^2$$

$$\Sigma_i \equiv 2\left[\frac{1+|R_i|^2}{1-|R_i|^2}\right] = A_i^2 + B_i^2 + C_i^2 + D_i^2$$

$$A_i^2 = a^2 w_i^2 + b^2 y_i^2 + 2abw_i y_i$$

$$C_i^2 = c^2 w_i^2 + d^2 y_i^2 + 2cdw_i y_i$$

$$B_i^2 = a^2 x_i^2 + b^2 z_i^2 + 2abx_i z_i$$

$$D_i^2 = c^2 x_i^2 + d^2 z_i^2 + 2cdx_i z_i$$

(INDEPENDENTLY AT EACH Q)

$$\Sigma_i = \overbrace{(w_i^2 + x_i^2)}^{\text{REF}}\alpha + \overbrace{(y_i^2 + z_i^2)}^{\text{REF}}\beta + 2\overbrace{(w_i y_i + x_i z_i)}^{\text{REF}}\gamma$$

SOLVE FOR UNKNOWNS $\alpha, \beta,$ AND γ TO GET

$i = 1, 2, 3$

$\alpha = a^2 + c^2$

$\beta = b^2 + d^2$

$\gamma = ab + cd$

$$R_{\text{UNKNOWN}} = \frac{(\beta - \alpha) - 2i\gamma}{2 + \beta + \alpha}$$

Bibliography

For SANS in the dilute solution limit, see Susan Krueger's presentation slides of her lecture in this series and/or D.I. Svergun and M.H.J. Koch, "Small-angle scattering studies of biological macromolecules in solution", *Reports on Progress in Physics* **66**, (2003) pgs. 1735-1782.

For phase-sensitive specular neutron reflectometry, see lecture notes (and references therein) on neutron reflectometry from the National School on X-Ray and Neutron Scattering, June 2014, Oak Ridge National Laboratory -- file can be downloaded from

http://ncnr.nist.gov/staff/chuck

file name

xns_nr_2014_majkrzak.pdf

KUNGL. VETENSKAPS-AKADEMIEN
THE ROYAL SWEDISH ACADEMY OF SCIENCES

THE NOBEL PRIZE IN CHEMISTRY 2014

POPULAR SCIENCE BACKGROUND

How the optical microscope became a nanoscope

Eric Betzig, Stefan W. Hell *and* ***William E. Moerner*** *are awarded the Nobel Prize in Chemistry 2014 for having bypassed a presumed scientific limitation stipulating that an optical microscope can never yield a resolution better than 0.2 micrometres. Using the fluorescence of molecules, scientists can now monitor the interplay between individual molecules inside cells; they can observe disease-related proteins aggregate and they can track cell division at the nanolevel.*

Red blood cells, bacteria, yeast cells and spermatozoids. When scientists in the 17th century for the first time studied living organisms under an optical microscope, a new world opened up before their eyes. This was the birth of microbiology, and ever since, the optical microscope has been one of the most important tools in the life-sciences toolbox. Other microscopy methods, such as electron microscopy, require preparatory measures that eventually kill the cell.

Glowing molecules surpassing a physical limitation

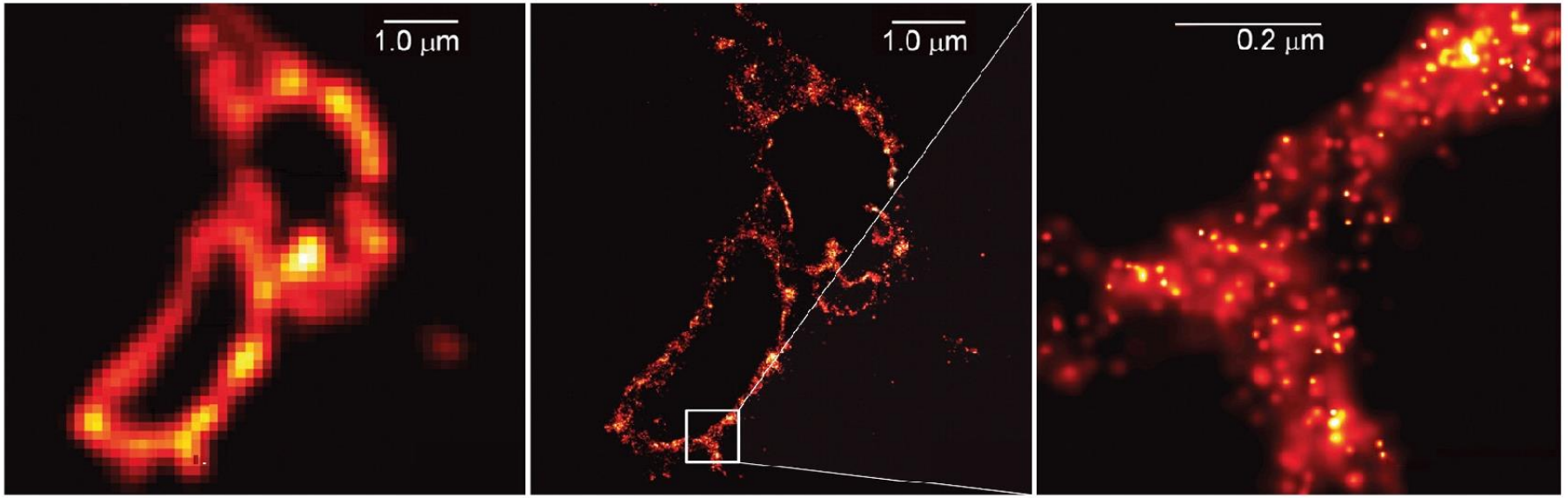

Figure 5. The centre image shows lysosome membranes and is one of the first ones taken by Betzig using single-molecule microscopy. To the left, the same image taken using conventional microscopy. To the right, the image of the membranes has been enlarged. Note the scale division of 0.2 micrometres, equivalent to Abbe's diffraction limit. The resolution is many times improved. Image from *Science* 313:1642–1645.